Available online at www.sciencedirect.com
ScienceDirect
Neuroscience Research 56 (2006) 61–72
Neuroscience Research
www.elsevier.com/locate/neures

Human astrocytes express 14-3-3 sigma in response to oxidative and DNA-damaging stresses

Jun-ichi Satoh [a,b,*], Hiroko Tabunoki [a], Yusuke Nanri [b], Kunimasa Arima [c], Takashi Yamamura [b]

[a] *Department of Bioinformatics and Neuroinformatics, Meiji Pharmaceutical University, 2-522-1 Noshio, Kiyose, Tokyo 204-8588, Japan*
[b] *Department of Immunology, National Institute of Neuroscience, NCNP, 4-1-1 Ogawahigashi, Kodaira, Tokyo 187-8502, Japan*
[c] *Department of Neuropathology, National Center Hospital for Mental, Nervous, and Muscular Disorders, NCNP, 4-1-1 Ogawahigashi, Kodaira, Tokyo 187-8502, Japan*

Received 5 March 2006; accepted 17 May 2006
Available online 23 June 2006

Abstract

The 14-3-3 protein family consists of seven isoforms, most of which are expressed abundantly in neurons and glial cells, although the σ isoform, a p53 target gene originally identified as an epithelium-specific marker, has not been identified in the human central nervous system. Here, we show that human astrocytes in culture expressed 14-3-3σ under stress conditions. By Western blot, the expression of 14-3-3σ, p53 and p21 was coordinately upregulated in astrocytes following exposure to hydrogen peroxide, 4-hydroxy-2-nonenal (4-HNE) or etoposide, a topoisomerase II inhibitor. 14-3-3σ was induced by treatment with 5-aza-2′-deoxycytidine, suggesting a hypermethylated status of the gene promoter in astrocytes. In vivo, a small subset of hypertrophic reactive astrocytes, often showing a multinucleated morphology, expressed 14-3-3σ in active demyelinating lesions of multiple sclerosis (MS) and ischemic lesions of cerebral infarction, where the expression of 4-HNE and 8-hydroxy-2′-deoxyguanosine was enhanced in reactive astrocytes. Microarray analysis of etoposide-treated astrocytes verified upregulation of p53-responsive genes and concurrent downregulation of mitotic checkpoint-regulatory genes. These observations suggest that 14-3-3σ might serve as a marker of oxidative and DNA-damaging stresses inducing the mitotic checkpoint dysfunction in reactive astrocytes under pathological conditions.

Keywords: Astrocytes; DNA damage; 14-3-3 Sigma; Multiple sclerosis; Multinucleated morphology; p53

1. Introduction

The 14-3-3 protein family consists of evolutionarily conserved, acidic 30-kDa proteins composed of seven isoforms named β, γ, ε, ζ, η, θ and σ in mammalian cells. A homodimeric or heterodimeric complex composed of the same or distinct isoforms constitutes a large cup-like structure possessing an amphipathic groove with two ligand-binding capacity (Fu et al., 2000). The dimeric complex acts as a molecular adaptor that interacts in a phosphorylation-dependent manner with key signaling molecules involved in cell differentiation, proliferation, transformation and apoptosis. The 14-3-3 protein regulates the function of target proteins by restricting their subcellular location, bridging them to modulate catalytic activity and protecting them from dephosphorylation or proteolysis, although 14-3-3 has some isoform-specific functions (MacKintosh, 2004). The 14-3-3 protein is expressed most abundantly in neurons in the central nervous system (CNS), where it represents 1% of total cytosolic proteins. Aberrant expression and impaired function of 14-3-3 in the CNS are associated with pathogenetic mechanisms of Creutzfeldt-Jacob disease, Alzheimer disease, Parkinson disease, spinocerebellar ataxia, amyotrophic lateral sclerosis and multiple sclerosis (MS) (Zerr et al., 1998; Chen et al., 2003; Satoh et al., 2004; review for Berg et al., 2002).

Oxidative stress-induced damage of nucleic acids, proteins and lipids plays a crucial role in the pathogenesis of neurodegenerative diseases, cerebral ischemia and MS, in

* Corresponding author. Tel.: +81 42 495 8678; fax: +81 42 495 8678.
E-mail address: satoj@my-pharm.ac.jp (J.-i. Satoh).

0168-0102/$ – see front matter
doi:10.1016/j.neures.2006.05.007

which activated macrophages/microglia serve as a major source of reactive oxygen and nitrogen intermediates (Smith et al., 1999). The cellular response to DNA damage is controlled by the cell cycle checkpoint function. Upon DNA-damaging insults, the cells rapidly arrest at two distinct cell cycle checkpoints; at the transition from G1 to S phase (G1 checkpoint) or from G2 to M phase (G2 checkpoint) to inhibit DNA replication and mitosis, until damaged DNA is properly repaired (Zhou and Elledge, 2000).

The 14-3-3σ isoform is originally identified as an epithelium-specific marker named stratifin (Leffers et al., 1993). The regulatory region of 14-3-3σ gene has two sets of the consensus sequence for binding of p53, a central regulator of DNA damage responses called "guardian of the genome" (Hoh et al., 2002). 14-3-3σ acts as a key component of the G2 checkpoint machinery, while cyclin-dependent kinase inhibitor 1A (CDKN1A) named p21, a prototype p53-responsive gene, regulates both G1 and G2 checkpoints (Chan et al., 1999). Exposure of the cells to DNA-damaging agents results in p53-dependent induction of 14-3-3σ, which in turn arrests the cells in the G2/M phase of cell cycle to allow the repair of damaged DNA, by sequestering the cdc2-cyclin B1 complex in the cytoplasm (Hermeking et al., 1997; Chan et al., 1999). 14-3-3σ-deficient cells incapable of maintaining the cell-cycle arrest undergo cell death as they enter mitosis (Chan et al., 1999). Since 14-3-3σ acts as a negative regulator of the cell cycle, epigenetic silencing of the 14-3-3σ gene by hypermethylation of the CpG-rich promoter region causes malignant transformation of the cells (Ferguson et al., 2000). Furthermore, 14-3-3σ is regulated at a protein level by activating a proteasome-dependent mechanism (Urano et al., 2002). Downregulation of 14-3-3σ allows human epidermal keratinocytes to escape replicative senescence (Dellambra et al., 2000).

At present, biological and pathological roles of 14-3-3σ in the CNS remain unknown. A previous study showed that the σ isoform is undetectable in the human CNS (Nakajima et al., 2003). Another study indicates that it is expressed in Pick bodies and human hippocampal neurons (Umahara et al., 2004). Here, we show that human astrocytes in culture express 14-3-3σ in response to oxidative and DNA-damaging stresses that upregulate p53 and p21. In vivo, 14-3-3σ is identified in a small subset of multinucleated hypertrophic reactive astrocytes in demyelinating lesions of MS and ischemic lesions of cerebral infarction, associated with enhanced oxidative stress and DNA damage responses. Our observations suggest that 14-3-3σ serves as a marker of oxidative and DNA-damaging stresses causing the mitotic checkpoint dysfunction in reactive astrocytes.

2. Materials and methods

2.1. Human astrocytes in culture

Human astrocytes were established from neuronal progenitor (NP) cells in culture as described previously (Satoh et al., 2004). NP cells isolated from the brain of a human fetus at 18.5 weeks gestation were obtained from BioWhittaker (Walkersville, MD). NP cells plated on a polyethyleneimine-coated surface were incubated in DMEM/F-12 medium (Invitrogen, Carlsbad, CA) containing an insulin-transferrin-selenium (ITS) supplement (Invitrogen), 20 ng/ml recombinant human epidermal growth factor (Higeta, Tokyo, Japan), 20 ng/ml recombinant human basic fibroblast growth factor (PeproTech EC, London, UK) and 10 ng/ml recombinant human leukemia inhibitory factor (Chemicon, Temecula, CA), according to the methods described previously (Carpenter et al., 1999). For the induction of astrocyte differentiation, NP cells were incubated for several weeks in DMEM (Invitrogen) supplemented with 10% fetal bovine serum (FBS), 100 U/ml penicillin and 100 μg/ml streptomycin (feeding medium). This incubation induced vigorous proliferation and differentiation of astrocytes accompanied by a rapid reduction in non-astroglial cell types. Their purity exceeded 98% by glial fibrillary acidic protein (GFAP) immunocytochemistry. DNA sequencing analysis verified that the p53 sequence of human astrocytes was identical to that of wild-type p53 (not shown).

2.2. Exposure of astrocytes to oxidative and DNA-damaging stresses

To load oxidative stress, astrocytes were incubated for 24 h in the serum-free DMEM/F-12 medium containing 10 or 100 μM hydrogen peroxide, a prototype oxidative stress inducer or in the feeding medium containing 20 μM 4-hydroxy-2-nonenal (4-HNE; Merck, Tokyo, Japan) dissolved in ethanol, a potent inducer of intracellular peroxide production (Uchida et al., 1999). To load DNA-damaging stress, the cells were incubated for varying periods in the feeding medium containing 20 μM etoposide (Sigma, St. Louis, MO) dissolved in DMSO, a topoisomerase II inhibitor that generates double-stranded DNA brakes. In some experiments, the serum-free culture supernatant was harvested and concentrated at an 1/85 volume by centrifugation on a Centricon-10 filter (Millipore, Bedford, MA).

To determine the methylation status of the 14-3-3σ promoter, astrocytes were incubated for 72 h in the feeding medium containing 5 μM 5-aza-2′-deoxycytidine (aza-dC; Sigma) dissolved in 50% acetic acid, a DNA methyltransferase inhibitor (Ferguson et al., 2000). Then, sodium bisulfite-treated genomic DNA was processed for methylation-specific PCR (MSP) analysis using the CpGenome DNA modification kit (Chemicon International) with the methylation status-specific primer sets listed in Table 1. To examine proteasome-dependent proteolysis of 14-3-3σ, astrocytes were incubated for 4 or 24 h in the feeding medium containing 10 μM MG-132 (Merck-Calbiochem), a proteasome inhibitor (Urano et al., 2004).

2.3. Western blot analysis

To prepare total protein extract, the cells were homogenized in RIPA lysis buffer composed of 50 mM Tris–HCl, pH 7.5, 150 mM NaCl, 1% Nonidet P40, 0.5% sodium deoxycholate, 0.1% SDS and a cocktail of protease inhibitors (Roche Diagnositics, Tokyo, Japan), followed by centrifugation at 12,000 rpm for 20 min at room temperature (RT). The supernatant was collected for separation on a 12% SDS-PAGE gel. The protein concentration was determined by a Bradford assay kit (BioRad, Hercules, CA). After gel electrophoresis, the protein was transferred onto nitrocellulose membranes and immunolabeled at RT overnight with the antibodies listed in Table 2. Then, the membranes were incubated at RT for 30 min with horseradish peroxidase (HRP)-conjugated anti-mouse, rabbit or goat IgG (Santa Cruz Biotechnology, Santa Cruz, CA). The specific reaction was visualized by using a chemiluminescent substrate (Pierce, Rockford, IL). After the antibodies were stripped by incubating the membranes at 50 °C for 30 min in stripping buffer composed of 62.5 mM Tris–HCl, pH 6.7, 2% SDS and 100 mM 2-mercaptoethanol, the membranes were processed for relabeling several times with different antibodies.

2.4. Microarray analysis

Five μg of total RNA, isolated from the cells by using TRIZOL reagent (Invitrogen), was in vitro amplified once and then cRNA was processed for analyzing a Whole Human Genome Oligonucleotide Microarray (G4112A, 41,000 genes; Agilent Technologies, Palo Alto, CA). The complete gene list is available online (http://www.chem.agilent.com/). To identify the genes whose expression was affected by DNA damage in cultured human astrocytes, cRNA isolated from the cells incubated for 24 h in the feeding medium containing 20 μM etoposide was labeled with a fluorescent dye Cy5, while cRNA of the

Table 1
Primers utilized for PCR analysis

Genes	GenBank accession no.	Sense primers	Antisense primers
14-3-3σ promoter (methylated)	AF029081	5′tggtagtttttatgaaaggcgtc3′	5′cctctaaccgcccaccacg3′
14-3-3σ promoter (unmethylated)	AF029081	5′atggtagtttttatgaaaggtgtt3′	5′ccctctaaccacccaccaca3′
14-3-3σ mRNA	NM_006142	5′tgcgagacaacctgacactgtgga3′	5′catactagtcctctcggcagggt3′
p53 mRNA	NM_000546	5′ttggaactcaaggatgcccaggct3′	5′tcagtctgagtcaggccctctgt3′
p21 mRNA	NM_078467	5′gcggcagaccagcatgacagattt3′	5′cagaagatgtagagcgggcctttg3′
GDF15 mRNA	NM_004864	5′gactgccactgcatatgagcagtc3′	5′tgtttgggcaggaatcgggtgtct3′
BIRC5 mRNA	NM_001168	5′ggctgcaccacttccagggtttat3′	5′cagaagcacctctggtgccacttt3′
ASPM mRNA	NM_018136	5′gcctctgatgtacgaagtaggtcc3′	5′ggaatgccaagcgtatccatcacc3′

The primer sets specific for methylated or unmethylated 14-3-3σ promoter were utilized for methylation-specific PCR analysis, while other primer sets were used for real-time PCR analysis. *Abbreviations*: GDF15, growth differentiation factor 15; BIRC5, bacuoviral IAP repeat-containing protein 5 (survivin); ASPM, abnormal spindle-like, microcephaly associated.

cells incubated for the same period in the medium supplemented with vehicle (DMSO) alone was labeled with Cy3. The array was hybridized at 60 °C for 17 h in the hybridization buffer containing equal amounts of Cy3- or Cy5-labeled cRNA. It was then scanned by the Agilent scanner (Agilent Technologies), and the data were analyzed by using the Feature Extraction software (Agilent Technologies). The fluorescence intensities (FI) of individual spots were quantified following global normalization between Cy3 and Cy5 signals, followed by Lowess normalization. The ratio of FI of Cy5 signal versus FI of Cy3 signal exceeding 2.0 was defined as significant upregulation, whereas the ratio smaller than 0.5 was considered as substantial downregulation.

2.5. Real-time RT-PCR analysis

DNase-treated total cellular RNA was processed for cDNA synthesis using oligo(dT)$_{12-18}$ primers and SuperScript II reverse transcriptase (Invitrogen). Then, cDNA was amplified by PCR in LightCycler ST300 (Roche Diagnostics) using SYBR Green I and the primer sets listed in Table 1. The levels of expression of target genes were standardized against those of the glyceraldehyde-3-phosphate dehydrogenase (G3PDH) gene detected in parallel in the identical cDNA samples. All the assays were performed in triplicate.

2.6. Human brain tissues

Ten micron-thick serial sections were prepared from autopsied brains of four MS patients and eight non-MS subjects. The tissues were fixed with 4% paraformaldehyde or 10% neutral formalin and embedded in paraffin. MS cases included a 29-year-old woman with secondary progressive MS (SPMS) who died of asphyxia, a 40-year-old woman with SPMS who died of respiratory failure, a 43-year-old woman with primary progressive MS (PPMS) who died of

Table 2
Primary antibodies utilized for immunohistochemistry and Western blot analysis

Antibodies (clones)	Suppliers	Code	Origin	Antigen specificity	Concentration used for immunohistochemistry	Concentration used for Western blotting
14-3-3 sigma	Immunobiological Laboratory	18642	Rabbit	14-3-3 sigma isoform	1 μg/ml	1 μg/ml
14-3-3 epsilon	Immunobiological Laboratory	18643	Rabbit	14-3-3 epsilon isoform	2 μg/ml	NA
p53 (DO-7)	Nichirei	413231	Mouse	Wild-type and mutant form of p53	Prediluted	Further diluted at 1:500
p21 (F-5)	Santa Cruz Biotechnology	sc-6246	Mouse	p21	0.4 μg/ml	0.2 μg/ml
4-HNE (HNEJ-2)	Japan Institute for the Control of Aging	MHN-20	Mouse	4-hydroxy-2-nonenal-modified proteins	2 μg/ml	NA
8-OHdG (N45.1)	Japan Institute for the Control of Aging	MOG-20P	Mouse	8-hydroxy-2'-deoxyguanosine	2 μg/ml	NA
GDF15	Santa Cruz Biotechnology	sc-10603	Goat	Intracellular proform of GDF15	2 μg/ml	0.1 μg/ml
GDF15	R & D Systems	AF957	Goat	Secreted mature form of GDF15	NA	0.1 μg/ml
GFAP	Dako	N1506	Rabbit	GFAP	Prediluted	NA
GFAP (GA5)	Nichirei	422261	Mouse	GFAP	Prediluted	NS
MBP	Dako	N1564	Rabbit	MBP	Prediluted	NA
NF (2F11)	Nichirei	412551	Mouse	Human 70-kDa and 200-kDa NF	Prediluted	NA
CD68 (KP1)	Dako	N1577	Mouse	CD68	Prediluted	NA
HSP60	Santa Cruz Biotechnology	sc-1052	Goat	HSP60	NA	0.1 μg/ml

Abbreviations: 4-HNE, 4-hydroxy-2-nonenal; 8-OHdG, 8-hydroxy-2′-deoxyguanosine; GDF15, growth differentiation factor 15; GFAP, glial fibrillary acidic protein; MBP, myelin basic protein; NF, neurofilament; HSP60, 60-kDa heat shock protein; NA, not applied.

hyperglycemia and a 33-year-old man with SPMS who died of sepsis. Detailed clinical and neuroradiological profiles of MS patients were described elsewhere (Satoh et al., 2004). Non-MS neurological and psychiatric disease cases included a 47-year-old man with acute cerebral infarction who died of sepsis, an 84-year-old man with acute cerebral infarction who died of disseminated intravascular coagulation, a 62-year-old man with old cerebral infarction who died of pancreatic cancer, a 56-year-old man with old cerebral infarction who died of myocardial infarction, a 36-year-old woman with schizophrenia who died of lung tuberculosis and a 61-year-old man with schizophrenia who died of asphyxia. Neurologically normal control cases included a 75-year-old woman who died of breast cancer and a 74-year-old woman who died of gastric and hepatic cancers. Autopsies on all subjects were performed at the National Center Hospital for Mental, Nervous and Muscular Disorders, National Center of Neurology and Psychiatry (NCNP), Tokyo, Japan. Written informed consent was obtained form all the cases. The present study was approved by the Ethics Committee of NCNP.

2.7. Immunohistochemistry

After deparaffination, tissue sections were heated in 10 mM citrate sodium buffer, pH 6.0, either by microwave at 95 °C for 10 min or by autoclave at 125 °C for 30 s in a temperature-controlled pressure chamber (Dako, Tokyo, Japan). They were treated at RT for 15 min with 3% hydrogen peroxide-containing methanol to block the endogenous peroxidase activity. The tissue sections were then incubated with phosphate-buffered saline (PBS) containing 10% normal goat serum or 10% normal rabbit serum at RT for 15 min to block non-specific staining. They were incubated in a moist chamber at 4 °C overnight with primary antibodies listed in Table 2. For 4-HNE and 8-hydroxy-2′-deoxyguanosine (8-OHdG) staining, the treatment with hydrogen peroxide-containing methanol was performed after immunolabeling with the primary antibodies to eliminate any potential effects caused by hydrogen peroxide-induced free radicals. The fine specificity of rabbit anti-14-3-3σ antibody (IBL, Gumma, Japan), mouse anti-4HNE monoclonal antibody (HNE-J2) and mouse anti-8OHdG monoclonal antibody (N45.1) was described elsewhere (Satoh et al., 2004; Toyokuni et al., 1995, 1997). After washing with PBS, the tissue sections were labeled at RT for 30 min with peroxidase-conjugated secondary antibodies (Nichirei, Tokyo, Japan), followed by incubation with a colorizing solution containing diaminobenzidine tetrahydrochloride (DAB) and a counterstain with hematoxylin. For negative controls, the tissue sections were incubated with a negative control reagent (Dako) instead of primary antibodies.

In some experiments, tissue sections were initially stained with mouse anti-GFAP monoclonal antibody (GA5, Nichirei), then followed by incubation with alkaline phosphatase-conjugated secondary antibody (Nichirei) and colorized with New Fuchsin substrate. After inactivation of the antibody by heating the sections by autoclave in 10 mM citrate sodium buffer, pH 6.0, they were relabeled with rabbit anti-14-3-3σ antibody (IBL), followed by incubation with peroxidase-conjugated secondary antibody (Nichirei) and colorized with DAB substrate.

3. Results

3.1. Human astrocytes in culture express 14-3-3σ in response to oxidative and DNA-damaging stresses

Cultured human astrocytes were exposed to hydrogen peroxide or 4-HNE, and then processed for Western blot analysis. Under baseline conditions, they expressed low levels of 14-3-3σ, p53 and p21 proteins (Fig. 1a and b, lane 1). The levels of 14-3-3σ, p53 and p21 were elevated markedly by a 24 h-exposure to 100 μM hydrogen peroxide or 20 μM 4-HNE (Fig. 1a, lane 3; Fig. 1b, lane 2), while the treatment with 10 μM hydrogen peroxide was ineffective (Fig. 1a, lane 2). Real-time RT-PCR analysis verified an oxidative stress-induced increase in 14-3-3σ and p21 mRNA levels (Fig. 2a, c and d). In contrast, an elevation of p53 protein levels in astrocytes by oxidative stress was not accompanied by a substantial increase of p53 mRNA levels, suggesting a major role of posttranscriptional regulation in p53 expression (Fig. 2b and e).

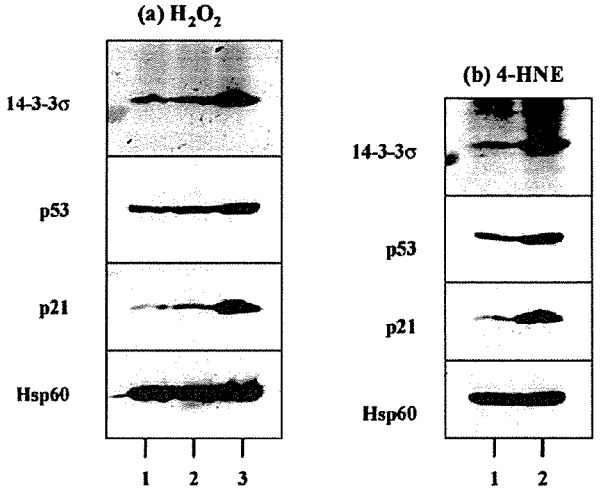

Fig. 1. The expression of 14-3-3σ, p53 and p21 in cultured human astrocytes following exposure to oxidative stress. Cultured human astrocytes were exposed for 24 h to two different oxidative stress-inducing stimuli. Then, they were studied by Western blot analysis of 14-3-3σ, p53, p21 and Hsp60 (a house-keeping gene product utilized as an internal control). The identical blot (150 μg of total cellular protein on each lane) was processed for sequential relabeling with different antibodies. (a) Hydrogen peroxide (H_2O_2) treatment. The lanes (1–3) indicate (1) untreated, (2) 10 μM hydrogen peroxide and (3) 100 μM hydrogen peroxide. (b) 4-Hydroxy-2-nonenal (4-HNE) treatment. The lanes (1 and 2) indicate treatment with (1) vehicle and (2) 20 μM 4-HNE.

Etoposide elevated greatly the levels of 14-3-3σ protein in cultured human astrocytes at 24 h after initiation of the treatment, while the elevation of p53 and p21 protein levels occurred much earlier, beginning at 4 h (Fig. 3a, lanes 1–6). Real-time RT-PCR analysis verified a great increase of 14-3-3σ mRNA but not of p53 mRNA in astrocytes exposed to etoposide (Fig. 2f and k). Treatment with aza-dC elevated markedly the protein levels of 14-3-3σ but not of p53 (Fig. 3b, lanes 1 and 2). Real-time RT-PCR analysis confirmed upregulation of 14-3-3σ mRNA in aza-dC-treated astrocytes (Fig. 2l). Methylation-specific PCR (MSP) analysis showed that an unmethylated DNA-specific PCR product was detected only when the cells were treated with aza-dC (Fig. 3d, lane 5). These observations indicate the constitutive hypermethylation of the 14-3-3σ promoter in astrocytes. MG-132 elevated the protein levels of p53 but not of 14-3-3σ, excluding a primary role of proteasome-dependent proteolysis in regulation of 14-3-3σ expression in cultured human astrocytes (Fig. 3c, lanes 1–3).

3.2. Multinucleated hypertrophic reactive astrocytes express 14-3-3σ in demyelinating lesions of MS and ischemic lesions of cerebral infarction

To identify astrocytes expressing 14-3-3σ in vivo in the human CNS, the brain, spinal cord and optic nerve sections of

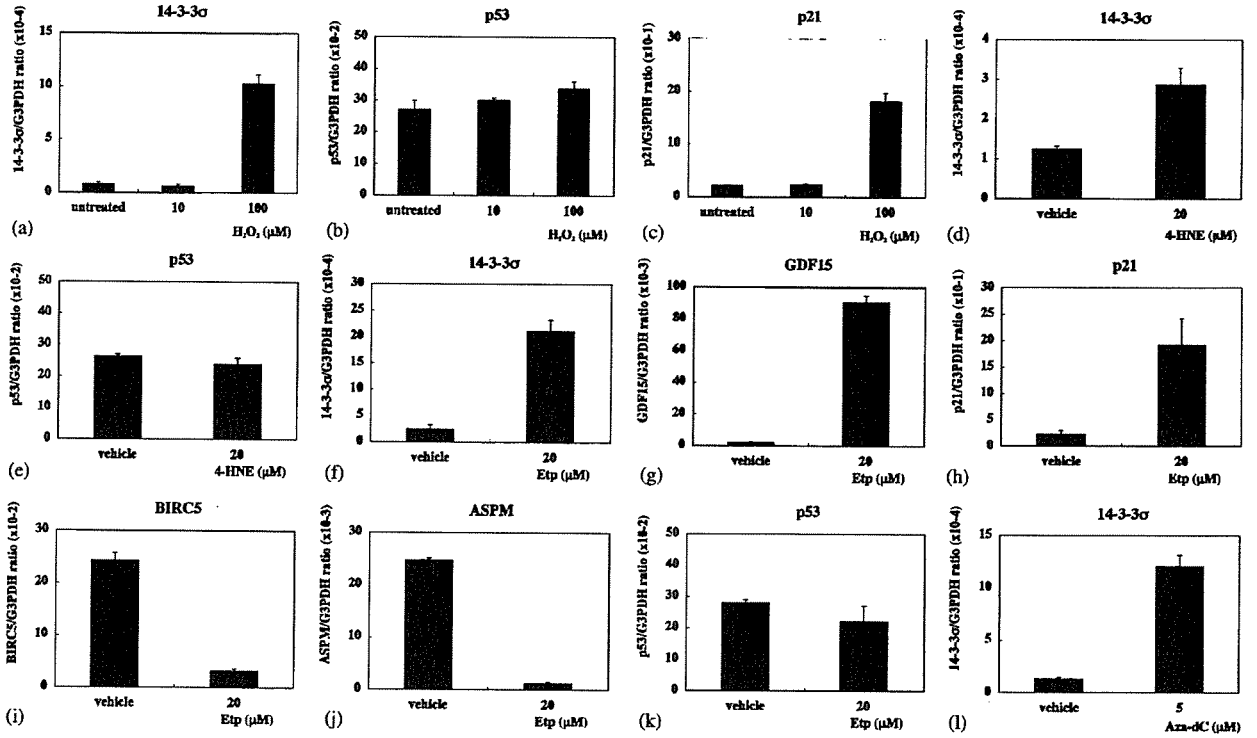

Fig. 2. The expression of 14-3-3σ, p53, p21, GDF15, BIRC5 and ASPM in cultured human astrocytes following exposure to oxidative and DNA-damaging stresses. Cultured human astrocytes were exposed for 24 h to (a–c) 10 to 100 μM hydrogen peroxide, (d and e) 20 μM 4-hydroxy-2-nonenal (4-HNE), (f–k) 20 μM etoposide (Etp) or (l) 5 μM 5-aza-2′-deoxycytidine (aza-dC). Then, they were processed for real-time RT-PCR analysis using the primer sets listed in Table 1. The expression levels of target genes were standardized against those of the glyceraldehyde-3-phosphate dehydrogenase (G3PDH) gene detected in the identical cDNA samples. The bar graph indicates mRNA levels of (a, d, f and l) 14-3-3σ, (b, e and k) p53, (c and h) p21, (g) GDF15, (i) BIRC5 and (j) ASPM.

four MS cases and eight non-MS cases were processed for immunohistochemistry using anti-14-3-3σ antibody. Serial sections were stained with the antibodies against GFAP, myelin basic protein (MBP), neurofilament (NF) proteins or CD68. In chronic active demyelinating lesions of MS, an intense 14-3-3σ immunolabeling was identified exclusively in a small subset of astrocytes, consisting of less than 0.1–1% of total GFAP$^+$ hypertrophic astrocytes, which often exhibited a binuclear or multinucleated morphology (Fig. 4a and b). Double-labeling immunohistochemistry verified coexpression of GFAP and 14-3-3σ in these astrocytes (Fig. 4f). In contrast, GFAP$^+$ glial scar was devoid of 14-3-3σ immunolabeling. As reported previously (Satoh et al., 2004), the great majority of reactive astrocytes, including those with a multinucleated morphology, also expressed a strong immunoreactivity for 14-3-3ε (Fig. 4c). In the brain of acute cerebral infarction, approximately 1–10% of reactive astrocytes expressed an intense 14-3-3σ immunoreactivity, some of which showed a binuclear morphology (Fig. 4d). The 14-3-3σ immunopositive cells often accumulated in the rim of necrotic core of infarcted lesions. The expression of 14-3-3σ in reactive astrocytes was less pronounced in the old lesions of cerebral infarction, and fairly weak or barely detectable in the brains of schizophrenia or neurologically normal control subjects, where most of the 14-3-3σ immunoreactive astrocytes were not multinuclear (Fig. 4e). Neither neurons, oligodendrocytes, macrophages/microglia, lymphocytes, endothelial cells nor ependymal cells expressed 14-3-3σ in the brains of any cases examined.

3.3. Reactive astrocytes express oxidative stress and DNA damage markers in demyelinating lesions of MS and ischemic lesions of cerebral infarction

Because 14-3-3σ is a p53 target gene, we investigated the expression of markers for oxidative stress and DNA damage responses in demyelinating lesions of MS and ischemic lesions of cerebral infarction. In all these lesions, the vast majority of reactive astrocytes including hypertrophic astrocytes with a multinucleated morphology, along with most of macrophages/microglia, expressed an intense immunoreactivity for 4-HNE, a marker of lipid peroxidation product (Fig. 5a and b). In addition, a subpopulation of neurons also expressed varying intensities of 4-HNE immunoreactivity in the brain of MS and non-MS cases (not shown). In demyelinating and ischemic lesions, less than 20% of reactive astrocytes expressed weak/intermediate immunolabeling for 8-OHdG, a marker of oxidative DNA damage (Fig. 5c). In contrast, reactive astrocytes expressing either 4-HNE or 8-OHdG were barely detectable in the brains of schizophrenia or neurologically normal control subjects (not shown). These results suggest that reactive astrocytes were exposed in vivo to oxidative stress and some of them expressed 14-3-3σ in these lesions.

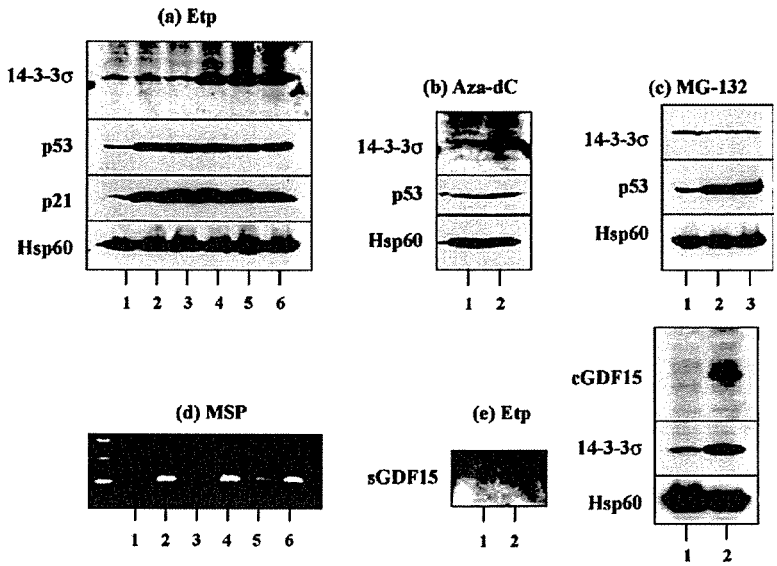

Fig. 3. The expression of 14-3-3σ, p53, p21 and GDF15 in cultured human astrocytes following exposure to etoposide, 5-aza-2′-deoxycytidine or MG-132. Cultured human astrocytes were exposed for varying periods to etoposide (Etp), 5-aza-2′-deoxycytidine (aza-dC) or MG-132. (a) Etp treatment: Western blot analysis of 14-3-3σ, p53, p21 and Hsp60 (internal control). The identical blot (150 μg of total cellular protein on each lane) was processed for sequential relabeling with different antibodies. The lanes (1–6) indicate (1) untreated, (2) 4 h, (3) 8 h, (4) 24 h, (5) 48 h and (6) 72 h after initiation of treatment with 20 μM Etp. (b) Aza-dC treatment: Western blot analysis of 14-3-3σ, p53 and Hsp60 (internal control). The identical blot (150 μg of total cellular protein on each lane) was processed for sequential relabeling with different antibodies. The lanes (1 and 2) indicate treatment with: (1) vehicle and (2) 5 μM aza-dC for 72 h. (c) MG-132 treatment: Western blot analysis of 14-3-3σ, p53 and Hsp60 (internal control). The identical blot was processed for sequential relabeling with different antibodies. The lanes (1–3) indicate (1) untreated, (2) 4 h and (3) 24 h after initiation of treatment with 10 μM MG-132. (d) Aza-dC treatment: Cultured human astrocytes were exposed for 72 h to 5 μM aza-dC or vehicle, then processed for methylation-specific PCR (MSP) analysis using the primer sets specific for methylated (M) or unmethylated (U) 14-3-3σ promoter listed in Table 1. The lanes (1–6) indicate (1) untreated, U primer, (2) untreated, M primer, (3) vehicle-treated, U primer, (4) vehicle-treated, M primer, (5) aza-dC-treated, U primer and (6) aza-dC-treated, M primer. (e) Etp treatment: Western blot analysis of GDF15, 14-3-3σ and Hsp60 (internal control). The panels represent the secreted mature form of GDF15 (sGDF15) detected in the concentrated culture supernatant (the left panel) and the intracellular proform of GDF15 (cGDF15) detected in the cellular protein extract (the right panel), derived from astrocytes exposed for 24 h to Etp or vehicle. In the right panel, the identical blot (150 μg of total cellular protein on each lane) was processed for sequential relabeling with different antibodies. The lanes (1 and 2) indicate treatment with (1) vehicle and (2) 20 μM etoposide.

3.4. Microarray analysis validated upregulation of p53-responsive genes and downregulation of mitotic checkpoint-regulatory genes in etoposide-treated astrocytes

To further obtain an insight into multinucleated reactive astrocytes overexpressing 14-3-3σ, a comprehensive gene expression profile of DNA-damaged astrocytes was studied by microarray analysis. Total RNA was isolated from human astrocytes in culture exposed for 24 h to either 20 μM etoposide or vehicle (DMSO). Among 41,000 genes on the microarray, 99 genes were upregulated over two-fold, whereas 396 genes were downregulated less than 0.5-fold following the treatment. Top 20 most markedly upregulated genes included 12 known p53-responsive genes, such as mouse double minute 2 homologue (MDM2), growth differentiation factor 15 (GDF15), p21, p53-induced protein 3 (PIG3), sestrin 1 (SESN1), hsp110-related gene (APG-1), adrenodoxin reductase (ADXR), p53-upregulated modulator of apoptosis (PUMA), nerve injury-induced protein ninjurin-1 (NINJ1), diacylglycerol kinase alpha (DGKA), tripartite motif-containing protein 22 (TRIM22) and transforming growth factor alpha (TGFA) (Table 3). Unexpectedly, a Cy5/Cy3 signal intensity ratio for 14-3-3σ was 1.77, which did not reach the levels of substantial upregulation defined as 2.0. Real-time RT-PCR analysis validated substantial upregulation of GDF15 and p21 mRNA in etoposide-treated astrocytes (Fig. 2g and h). Upregulation of GDF15 in astrocytes under DNA damaging stresses was supported by following observations. A secreted mature form of GDF15 (15-kDa) was identified in culture supernatant of etoposide-treated astrocytes but not of vehicle-treated cells (Fig. 3e, left panel, lanes 1 and 2). An intracellular proform of GDF15 (37-kDa) was expressed in etoposide-treated astrocytes but undetectable in vehicle-treated cells (Fig. 3e, right panel, lanes 1 and 2). A substantial population (1–10%) of reactive astrocytes and macrophages/microglia expressed a weak/intermediate GDF15 immunoreactivity in chronic active demyelinating lesions of MS (Fig. 5d) and ischemic lesions of acute and old cerebral infarction (not shown).

Top 20 most profoundly downregulated genes in etoposide-treated astrocytes included a battery of the genes involved in cell cycle regulation, particularly those essential for the mitotic checkpoint function. They are composed of abnormal spindle-like, microcephaly associated (ASPM), budding uninhibited by benzimidazoles 1 homolog (BUB1), kinetochore associated protein 2 (KNTC2), actin-binding protein anillin (ANLN), baculoviral IAP repeat-containing protein 5 (BIRC5), centromere protein F (CENPF), kinesin family member 11 (KIF11) and 20A (KIF20A), T-LAK cell-originated protein kinase

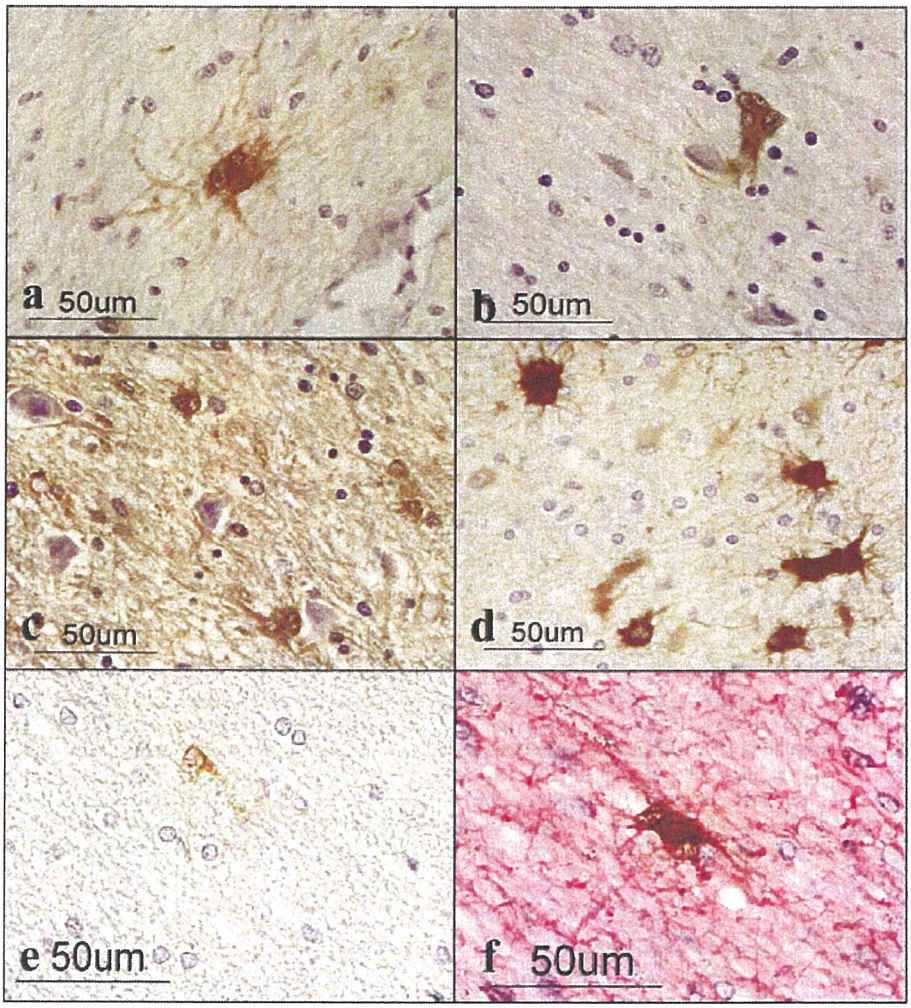

Fig. 4. The expression of 14-3-3σ in a subset of multinucleated hypertrophic reactive astrocytes in demyelinating lesions of MS and ischemic lesions of cerebral infarction. The tissue sections of MS and non-MS brains were studied by immunohistochemistry. (a) 14-3-3σ immunolabeling: Chronic active demyelinating lesions in optic nerve of a 33 year-old man with SPMS. A multinucleated hypertrophic cell is intensely stained. (b) 14-3-3σ immunolabeling: Chronic active demyelinating lesions in pons of the same case as (a). A multinucleated hypertrophic cell is intensely stained. (c) 14-3-3ε immunolabeling: Chronic active demyelinating lesions in pons of the case same as (a). Several binuclear hypertrophic cells are intensely stained. (d) 14-3-3σ immunolabeling: The rim of necrotic core in the parietal cerebral cortex of a 47 year-old man with acute cerebral infarction. Numerous binuclear hypertrophic cells are intensely stained. (e) 14-3-3σ immunolabeling: The frontal cortex of a neurologically normal 74-year-old woman who died of gastric and hepatic cancers. A single-nuclear cell is weakly stained. (f) 14-3-3σ and GFAP double immunolabeling: Chronic active demyelinating lesions in optic nerve of the same case of (a). A binuclear hypertrophic cell shows an intense immunoreactivity for both 14-3-3σ (brown) and GFAP (red). Glial scar that covers demyelinating lesions also expresses GFAP (red).

(TOPK), lamin B1 (LMNB1) and MAD2 mitotic arrest deficient-like 1 (MAD2L1) (Table 4). Real-time RT-PCR analysis verified substantial downregulation of ASPM and BIRC5 mRNA in etoposide-treated astrocytes (Fig. 2i and j).

4. Discussion

The present study for the first time showed that human astrocytes in culture expressed 14-3-3σ in response to oxidative and DNA-damaging stresses. Furthermore, a subset of reactive astrocytes, but no other cell types, intensely expressed 14-3-3σ in chronic active demyelinating lesions of MS and acute ischemic lesions of cerebral infarction. Importantly, 14-3-3σ-expressing astrocytes often exhibited a multinucleated hypertrophic morphology that might represent an unusual state of nuclear division without cytokinesis.

Several previous studies reported an accumulation of multinucleated reactive astrocytes in chronic demyelinating lesions of MS (Schlote, 1975; Nishie et al., 2004). We found that many reactive astrocytes expressed 4-HNE and 8-OHdG, oxidative stress and DNA damage response markers in demyelinating lesions of MS and ischemic lesions of infarction. In accordance with our observations, reactive astrocytes metabolize 4-HNE-modified low density lipoprotein in demyelinating lesions of MS (Newcombe et al., 1994). Oxidative DNA damage accumulates in chronic active MS plaques (Vladimirova et al., 1998; Lu et al., 2000). We recently found that MS lymphocytes show a gene expression profile

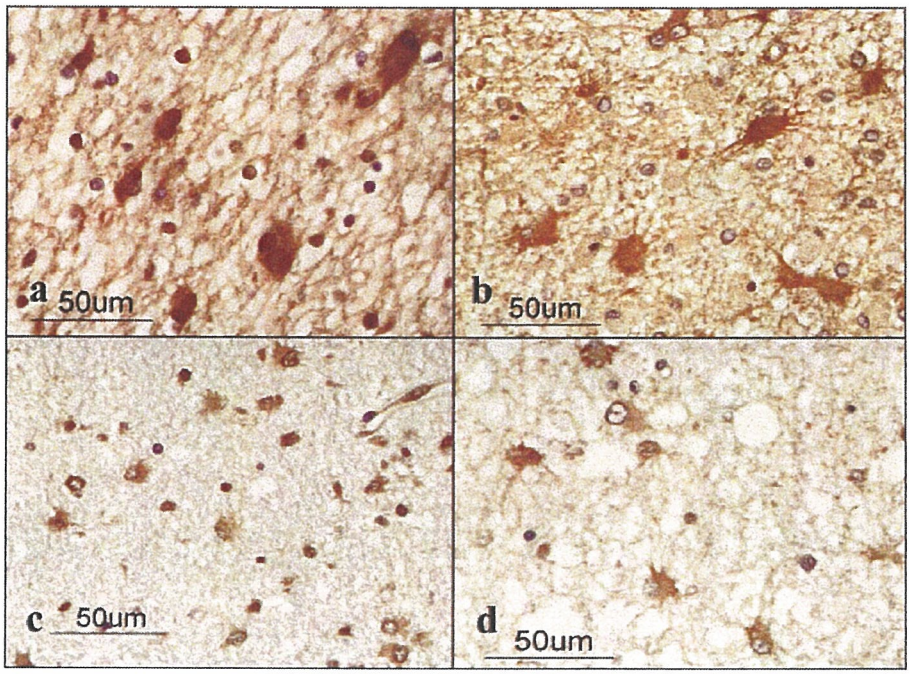

Fig. 5. The expression of oxidative stress and DNA damage response markers in reactive astrocytes in demyelinating lesions of MS and ischemic lesions of cerebral infarction. The tissue sections of MS and non-MS brains were studied by immunohistochemistry. (a) 4-HNE immunolabeling: Chronic active demyelinating lesions in optic nerve of a 40-year-old woman with SPMS. Numerous binuclear hypertrophic cells are intensely stained. (b) 4-HNE immunolabeling: The rim of necrotic core in the parietal cerebral cortex of a 47-year-old man with acute cerebral infarction. Numerous cells morphologically compatible with hypertrophic reactive astrocytes are intensely stained. (c) 8-Hydroxy-2′-deoxyguanosine (8-OHdG) immunolabeling: Chronic active demyelinating lesions in the parietal cerebral cortex of a 33-year-old man with SPMS. Numerous cells morphologically compatible with reactive astrocytes and microglia are moderately stained. (d) GDF15 immunolabeling: Chronic active demyelinating lesions in the frontal cerebral cortex of the same case as (a). Numerous cells morphologically compatible with hypertrophic reactive astrocytes are moderately stained.

representing a counterbalance between promoting and preventing apoptosis and DNA damage (Satoh et al., 2005). All of these observations propose a pivotal role of oxidative and DNA-damaging stresses in the pathological process of MS.

Demethylating treatment with aza-dC upregulated 14-3-3σ expression in cultured human astrocytes. Because epigenetic silencing of the 14-3-3σ gene causes malignant transformation of various cell types (Ferguson et al., 2000; Kaneuchi et al., 2004), it is surprising that the 14-3-3σ promoter region is constitutively hypermethylated in non-transformed astrocytes we utilized. However, a recent study showed that the 14-3-3σ promoter is methylated physiologically to some degree in normal lymphocytes (Bhatia et al., 2003). 14-3-3σ protein levels are also regulated by proteasome-dependent proteolytic degradation in certain cell types. Efp, an estrogen-inducible RING-finger-dependent ubiquitin ligase E3, targets proteolysis of 14-3-3σ in breast cancer cells (Urano et al., 2002). The 14-3-3σ protein expression is upregulated in Efp-deficient cells that show a reduced cell growth rate, and is elevated in human prostate cancer cells by treatment with MG-132, a proteasome inhibitor (Urano et al., 2004). In contrast, we found that MG-132 did not alter the 14-3-3σ protein levels, excluding an active involvement of proteasome-dependent regulation in human astrocytes under standard culture conditions. On the contrary, MG-132 elevated the p53 protein levels in astrocytes, supporting a major role of posttranslational modifications in the stability of p53 protein (Slee et al., 2004). Following exposure to etoposide, p53 and p21 protein levels were elevated much earlier than the levels of 14-3-3σ in astrocytes. The difference in induction kinetics between p53 and 14-3-3σ looks unusual, because 14-3-3σ is located at the point immediately downstream of p53. However, delayed induction of 14-3-3σ was observed in several cell types (Zhao et al., 2000).

The most markedly upregulated genes in etoposide-treated astrocytes included 12 known p53-regulated genes that have the p53-binding consensus site in the regulatory region. Among them, MDM2 with an E3 ubiquitin ligase activity acts as a negative regulator of p53. MDM2 interacts with p53, inhibits transactivation by p53 and targets p53 for proteasomal degradation (Meek, 2004). In contrast, 14-3-3σ has a positive feedback effect on p53 regulation. 14-3-3σ facilitates the tetramerization of p53, enhances the transcriptional activity of p53 and antagonizes the function of MDM2 by blocking MDM2-mediated ubiquitination and nuclear export of p53 (Yang et al., 2003).

In the present study, there exists an apparent disagreement in the levels of 14-3-3σ expression in etoposide-treated astrocytes among microarray, real-time RT-PCR and Western blot. The Cy5/Cy3 signal intensity ratio for 14-3-3σ (1.77) in microarray did not reach the levels of substantial upregulation defined as 2.0, while the etoposide-induced elevation of 14-3-3σ levels was more evident in real-time RT-PCR (an 11.4-fold increase,

Table 3
Top 20 upregulated genes in cultured human astrocytes following treatment with etoposide

No.	Cy5/Cy3 signal intensity ratio	Gene symbol	Gene name	Unigene	Function	p53-responsive genes
1	7.36	MDM2	Mouse double minute 2 homologue	Hs.212217	A nuclear phosphoprotein with E3 ubiquitin ligase activity that inhibits transactivation by p53 and targets p53 for proteasomal degradation	Yes
2	7.04	GDF15	Growth differentiation factor 15, macrophage-inhibiting cytokine 1 (MIC1), placentral transforming growth factor-beta (PTGFβ)	Hs.296638	A member of TGFβ superfamily that regulates tissue differentiation and maintenance	Yes
3	6.75	CDKN1A	Cyclin-dependent kinase inhibitor 1A (p21)	Hs.370771	A cyclin-dependent kinase inhibitor that acts as a regulator of cell cycle progression at G1 and G2 checkpoints	Yes
4	5.33	TP53I3	Tumor protein p53 inducible protein 3, p53-induced gene 3 (PIG3)	Hs.50649	A quinone oxidoreductase involved in oxidative stress-induced apoptosis by p53	Yes
5	4.17	HAS3	Hyaluronan synthase 3	Hs.85962	A member of the HAS gene family that synthesizes the extracellular matrix component hyaluronan	Unreported
6	4.17	INPP5D	Inositol polyphosphate-5-phosphatase, SH2-containing inositol phosphatase (SHIP)	Hs.262886	An enzyme that acts as a negative regulator of cytokine signal transduction	Unreported
7	3.93	SESN1	Sestrin 1	Hs.14125	A protein of the GADD family that provides antixidant defense	Yes
8	3.46	CPE	Carboxypeptidase E	Hs.75360	An enzyme involved in the biosynthesis of peptide hormones and neurotransmitters	Unreported
9	3.41	APG-1	Hsp110-related gene apg-1, osmotic stress protein of 94-kDa Osp94	Hs.135554	A protein of the HSP110 family upregulated by hypertonic and heat stresses	Yes
10	3.41	ADXR	Adrenodoxin reductase	Hs.69745	A mitochondrial flavoprotein that initiates electron transport for cytochrome P450	Yes
11	3.39	APOBEC3C	Apolipoprotein B mRNA editing enzyme, catalytic polypeptide-like 3C	Hs.441124	A member of the cytidine deaminase gene family that shows potent DNA mutator activity	Unreported
12	3.33	BBC3	BCL2-binding component 3, p53-upregulated modulator of apoptosis (PUMA)	Hs.87246	A member of BH3-only Bcl-2 family that acts as an essential mediator of p53-dependent apoptosis	Yes
13	3.21	RDH10	Retinol dehydrogenase 10	Hs.244940	An enzyme that generates all-trans retinal from all-trans retinol involved in the photic visual cycle	Unreported
14	3.17	DYRK3	Dual-specificity tyrosine phosphorylation-regulated kinase 3	Hs.164267	A dual-specificity protein kinase of the DYRK family that catalyzes phosphorylation of histone H2B	Unreported
15	3.16	NINJ1	Nerve injury-induced protein, ninjurin 1	Hs.11342	A cell surface protein that acts as a homophilic adhesion molecule upregulated by nerve injury	Yes
16	3.06	DGKA	Diacylglycerol kinase, alpha 80-kDa	Hs.172690	A member of the diacylglycerol kinase family that competes with protein kinase C for the second messenger diacylglycerol	Yes
17	3.05	TRIM22	Tripartite motif-containing protein 22	Hs.318501	An interferon-induced member of the tripartite motif family involved in antiviral action of interferons	Yes
18	3.02	CES2	Carboxylesterase 2	Hs.282975	An enzyme that hydrolyzes ester groups of drugs and toxins	Unreported
19	2.95	APOBEC3F	Apolipoprotein B mRNA editing enzyme, catalytic polypeptide-like 3F	Hs.337667	A member of the cytidine deaminase gene family that inhibits HIV-1 infectivity	Unreported
20	2.92	TGFA	Transforming growth factor, alpha	Hs.170009	A mitogenic growth factor that competes with EGF for binding to the EGF receptor	Yes

Whole human genome microarray (41,000 genes) was hybridized with Cy5-labeled cRNA isolated from etoposide-treated astrocytes and Cy3-labeled cRNA of those treated with vehicle. Among 99 genes upregulated in etoposide-treated astrocytes, top 20 most greatly upregulated and annotated genes are listed in order of the Cy5/Cy3 signal intensity ratio. The results of GDF15 and CDKN1A (p21) (underlined) were validated by real-time RT-PCR analysis shown in Fig. 2g and h.

Table 4
Top 20 downregulated genes in cultured human astrocytes following treatment with etoposide

No.	Cy5/Cy3 signal intensityratio	Gene symbol	Gene name	Unigene	Function
1	0.11	ASPM	Abnormal spindle-like, microcephaly associated	Hs.121028	A protein that regulates mitotic spindle activity in neuronal progenitor cells
2	0.12	UHRF1	Ybiquitin-like protein containing PHD and RING finger domains 1	Hs.108106	A nuclear phosphoprotein that regulates transcription of topoisomerase II-alpha
3	0.12	BUB1	BUB1 budding uninhibited by benzimidazoles 1 homolog	Hs.287472	A kinase involved in mitotic checkpoint function
4	0.13	MKI67	Proliferation-related Ki-67 antigen	Hs.80976	A nuclear antigen expressed in proliferating cells
5	0.14	KNTC2	Kinetochore associated protein 2	Hs.414407	A protein involved in spindle checkpoint function required for correct segregation of chromosomes during cell division
6	0.15	DLG7	Discs, large homolog 7	Hs.77695	A cell cycle regulator that plays a role in the carcinogenesis
7	0.16	ANLN	Actin-binding protein, anillin	Hs.62180	An actin binding-protein that acts as a cleavage furrow protein required for cytokinesis
8	0.16	BIRC5	Baculoviral IAP repeat-containing protein 5 (survivin)	Hs.1578	A member of the IAP gene family that prevents apoptotic cell death
9	0.16	CENPF	Centromere protein F	Hs.77204	A protein that associates with the centromere-kinetochore complex involved in chromosome segregation during mitosis
10	0.17	KIF11	Kinesin family member 11	Hs.8878	A motor protein of the kinesin-like protein family that plays a role in mitotic spindle dynamics
11	0.17	MELK	Maternal embryonic leucine zipper kinase	Hs.184339	A serine/threonine kinase that regulates the G2/M progression of the cell cycle by phosphorylating CDC25B
12	0.17	TOPK	T-LAK cell-originated protein kinase, PDZ binding kinase (PBK)	Hs.104741	A serine/threonine kinase that plays a role in phosphorylation events during mitosis
13	0.17	KIF20A	Kinesin family member 20A	Hs.73625	A microtubule-associated motor protein that plays a role in intracellular transport and cell division
14	0.18	LMNB1	Lamin B1	Hs.89497	A member of the intermediate filament protein family that consitutes a major component of the nuclear lamina
15	0.18	ARHGAP11A	Rho GTPase activating protein 11 A	Hs.172652	A Rho GTPase-activating protein (GAP)
16	0.19	TOP2A	DNA topoisomerase II alpha	Hs.156346	A DNA topoisomerase that regulates the topologic states of DNA during transcription
17	0.19	MAD2L1	MAD2 mitotic arrest deficient-like 1	Hs.79078	A component of the mitotic spindle assemby checkpoint required for the completion of chromosome-microtubule attachment during metaphase
18	0.19	MCM6	Minichromosome maintenance deficient 6	Hs.444118	A DNA licensing factor essential for the initiation of genome replication
19	0.19	SHCBP1	SHC SH2-domain binding protein 1	Hs.123253	A cytoplasmic protein that interacts with the Shc SH2 domain in a phosphotyrosine-independent manner
20	0.19	RACGAP1	Rac GTPase activating protein 1	Hs.505469	A GTPase-activating protein (GAP) for Rac and Cdc42

Whole human genome microarray (41,000 genes) was hybridized with Cy5-labeled cRNA isolated from etoposide-treated astrocytes and Cy3-labeled cRNA of those treated with vehicle. Among 396 genes downregulated in etoposide-treated astrocytes, top 20 most profoundly downregulated and annotated genes are listed in order of the Cy5/Cy3 signal intensity ratio. The results of ASPM and BIRC5 (underlined) were validated by real-time RT-PCR analysis shown in Fig. 2i and j.

Fig. 2f) and in Western blot (a 2.5-fold increase, Fig. 3a). These discrepancies are attributable to the differences in the basic principle (competitive hybridization and two-color detection in microarray versus individualized amplification and one-color detection in real-time RT-PCR, and antibody-based amplified immunodetection in Western blot), normalization (unbiased global normalization of all features in microarray versus normalization of selected genes against the levels of housekeeping genes in real-time RT-PCR and Western blot), linear amplification of RNA prior to microarray analysis and differential strategies in probe designs for microarray and real-time RT-PCR (Jenson et al., 2003; Wang et al., 2006), and in addition to potential posttranscriptional regulation of 14-3-3σ on special occasions (Urano et al., 2002).

GDF15, alternatively named macrophage-inihibiting cytokine 1 (MIC1), is a secreted protein of the TGFβ superfamily. An intracellular proform of GDF15 is processed into a mature secreted form after proteolytic cleavage (Bootcov et al., 1997). GDF15 is transcriptionally activated by p53 following DNA damage, and overexpression of GDF15 induces G1 cell cycle arrest and apoptosis in human breast cancer cells (Li et al., 2000). GDF15, produced in response to injury by astrocytes, neurons, macrophages/microglia and choroid plexus epithelium, acts as a potent trophic factor for mesencephalic dopaminergic neurons in the CNS (Strelau et al., 2000; Schober et al., 2001). We showed that reactive astrocytes and macrophages/microglia expressed an immmunoreactivity for GDF15 in demyelinating lesions of MS and ischemic lesions of cerebral infarction, and GDF15 protein was secreted into the culture medium of human astrocytes, when the cells were exposed to etoposide.

The most profoundly downregulated genes in etoposide-treated astrocytes included a battery of mitotic checkpoint-regulatory genes. Among them, ASPM regulates mitotic spindle activity in neuronal progenitor cells, and a panel of protein-truncating mutations in the ASPM gene cause human autosomal recessive primary microcephaly (MCPH) (Bond et al., 2002). BUB1 is the human homolog of the *yeast* BUB1 gene, a kinase involved in mitotic checkpoint function. The mutational inactivation of BUB1 induces mitotic checkpoint defects and chromosomal instability in colorectal cancer cells (Cahill et al., 1998). KNTC2 regulates spindle checkpoint signaling required for correct segregation of chromosomes during cell division (Martin-Lluesma et al., 2002). BIRC5, also known as survivin, is a member of the IAP gene family expressed abundantly in the G2/M phase in a cell cycle-dependent manner, where it associates with microtubules of the mitotic spindle (Li et al., 1998). Although survivin has two putative p53-binding sites in the promoter region of BIRC5 (Mirza et al., 2002), it was downregulated in etoposide-treated astrocytes. Importantly, a set of p53-responsive genes are repressed by p53 via an as yet unidentified mechanism (Mirza et al., 2003). Since etoposide reduces the expression of mitotic checkpoint genes in cultured human astrocytes, we could propose a possible scenario that a small subset of hypertrophic reactive astrocytes with an enhanced expression of 14-3-3σ showed a multinucleated morphology due to aberrant regulation of the mitotic signaling pathway, following persistent exposure to oxidative and DNA-damaging stresses in demyelinating and ischemic lesions.

Acknowledgements

This work was supported by grants to J.-I.S. from Research on Psychiatric and Neurological Diseases and Mental Health, the Ministry of Health, Labour and Welfare of Japan (H17-020), Research on Health Sciences Focusing on Drug Innovation, the Japan Health Sciences Foundation (KH21101) and the Grant-in-Aid for Scientific Research, the Ministry of Education, Science, Sports and Culture (B18300118). All autopsied brain samples were obtained from Research Resource Network (RRN), Japan.

References

Berg, D., Holzmann, C., Riess, O., 2002. 14-3-3 proteins in the nervous system. Nat. Rev. Neurosci. 4, 752–762.

Bhatia, K., Siraj, A.K., Hussain, A., Bu, R., Gutiérrez, M.I., 2003. The tumor suppressor gene 14-3-3 σ is commonly methylated in normal and malignant lymphoid cells. Cancer Epidemiol. Biomarkers Prev. 12, 165–169.

Bond, J., Roberts, E., Mochida, G.H., Hampshire, D.J., Scott, S., Askham, J.M., Springell, K., Mahadevan, M., Crow, Y.J., Markham, A.F., Walsh, C.A., Woods, C.G., 2002. ASPM is a major determinant of cerebral cortical size. Nat. Genet. 32, 316–320.

Bootcov, M.R., Bauskin, A.R., Valenzuela, S.M., Moore, A.G., Bansal, M., He, X.Y., Zhang, H.P., Donnellan, M., Mahler, S., Pryor, K., Walsh, B.J., Nicholson, R.C., Fairlie, W.D., Por, S.B., Robbins, J.M., Breit, S.N., 1997. MIC-1, a novel macrophage inhibitory cytokine, is a divergent member of the TGF-β superfamily. Proc. Natl. Acad. Sci. U.S.A. 94, 11514–11519.

Cahill, D.P., Lengauer, C., Yu, J., Riggins, G.J., Willson, J.K., Markowitz, S.D., Kinzler, K.W., Vogelstein, B., 1998. Mutations of mitotic checkpoint genes in human cancers. Nature 392, 300–303.

Carpenter, M.K., Cui, X., Hu, Z.-Y., Jackson, J., Sherman, S., Seiger, Å., Wahlberg, L.U., 1999. In vitro expansion of a multipotent population of human neural progenitor cells. Exp. Neurol. 158, 262–278.

Chan, T.A., Hermeking, H., Lengauer, C., Kinzler, K.W., Vogelstein, B., 1999. 14-3-3σ is required to prevent mitotic catastrophe after DNA damage. Nature 401, 616–620.

Chen, H.-K., Fernandez-Funez, P., Acevedo, S.F., Lam, Y.C., Kaytor, M.D., Fernandez, M.H., Aitken, A., Skoulakis, E.M., Orr, H.T., Botas, J., Zoghbi, H.Y., 2003. Interaction of Akt-phosphorylated ataxin-1 with 14-3-3 mediates neurodegeneration in spinocerebellar ataxia type 1. Cell 113, 457–468.

Dellambra, E., Golisano, O., Bondanza, S., Siviero, E., Lacal, P., Molinari, M., D'Atri, S., De Luca, M., 2000. Downregulation of 14-3-3σ prevents clonal evolution and leads to immortalization of primary human keratinocytes. J. Cell Biol. 149, 1117–1129.

Ferguson, A.T., Evron, E., Umbricht, C.B., Pandita, T.K., Chan, T.A., Hermeking, H., Marks, J.R., Lambers, A.R., Fytreal, P.A., Stampfer, M.R., Sukumar, S., 2000. High frequency of hypermethylation at the 14-3-3 σ locus leads to gene silencing in breast cancer. Proc. Natl. Acad. Sci. U.S.A. 97, 6049–6054.

Fu, H., Subramanian, R.R., Masters, S.C., 2000. 14-3-3 proteins: structure, function, and regulation. Annu. Rev. Pharmacol. Toxicol. 40, 617–647.

Hermeking, H., Lengauer, C., Polyak, K., He, T.-C., Zhang, L., Thiagalingam, S., Kinzler, K.W., Vogelstein, B., 1997. 14-3-3σ is a p53-regulated inhibitor of G2/M progression. Mol. Cell 1, 3–11.

Hoh, J., Jin, S., Parrado, T., Edington, J., Levine, A.J., Ott, J., 2002. The p53MH algorithm and its application in detecting p53-responsive genes. Proc. Natl. Acad. Sci. U.S.A. 99, 8467–8472.

Jenson, S.D., Robetorye, R.S., Bohling, S.D., Schumacher, J.A., Morgan, J.W., Lim, M.S., Elenitoba-Johnson, K.S., 2003. Validation of cDNA microarray gene expression data obtained from linearly amplified RNA. J. Clin. Pathol. Mol. Pathol. 56, 307–312.

Kaneuchi, M., Sasaki, M., Tanaka, Y., Shiina, H., Verma, M., Ebina, Y., Nomura, E., Yamamoto, R., Sakuragi, N., Dahiya, R., 2004. Expression and methylation status of 14-3-3 sigma gene can characterize the different histological features of ovarian cancer. Biochem. Biophys. Res. Commun. 316, 1156–1162.

Leffers, H., Madsen, P., Rasmussen, H.H., Honoré, B., Andersen, A.H., Walbum, E., Vandekerckhove, J., Celis, J.E., 1993. Molecular cloning and expression of the transformation sensitive epithelial marker stratifin. A member of a protein family that has been involved in the protein kinase C signaling pathway. J. Mol. Biol. 231, 982–998.

Li, F., Ambrosini, G., Chu, E.Y., Plescia, J., Tognin, S., Marchisio, P.C., Altieri, D.C., 1998. Control of apoptosis and mitotic spindle checkpoint by survivin. Nature 396, 580–584.

Li, P.-X., Wong, J., Ayed, A., Ngo, D., Brade, A.M., Arrowsmith, C., Austin, R.C., Klamut, H.J., 2000. Placental transforming growth factor-β is a downstream mediator of the growth arrest and apoptotic response of tumor cells to DNA damage and p53 overexpression. J. Biol. Chem. 275, 20127–20135.

Lu, F., Selak, M., O'Connor, J., Croul, S., Lorenzana, C., Butunoi, C., Kalman, B., 2000. Oxidative damage to mitochondrial DNA and activity of mitochondrial enzymes in chronic active lesions of multiple sclerosis. J. Neurol. Sci. 177, 95–103.

MacKintosh, C., 2004. Dynamic interactions between 14-3-3 proteins and phosphoproteins regulate diverse cellular processes. Biochem. J. 381, 329–342.

Martin-Lluesma, S., Stucke, V.M., Nigg, E.A., 2002. Role of Hec1 in spindle checkpoint signaling and kinetochore recruitment of Mad1/Mad2. Science 297, 2267–2270.

Meek, D.W., 2004. The p53 response to DNA damage. DNA Repair 3, 1049–1056.

Mirza, A., McGuirk, M., Hockenberry, T.N., Wu, Q., Ashar, H., Black, S., Wen, S.F., Wang, L., Kirschmeier, P., Bishop, W.R., Nielsen, L.L., Pickett, C.B., Liu, S., 2002. Human survivin is negatively regulated by wild-type p53 and participates in p53-dependent apoptotic pathway. Oncogene 21, 2613–2622.

Mirza, A., Wu, Q., Wang, L., McClanahan, T., Bishop, W.R., Gheyas, F., Ding, W., Hutchins, B., Hockenberry, T., Kirschmeier, P., Greene, J.R., Liu, S., 2003. Global transcriptional program of p53 target genes during the process of apoptosis and cell cycle progression. Oncogene 22, 3645–3654.

Nakajima, T., Shimooka, H., Weixa, P., Segawa, A., Motegi, A., Jian, Z., Masuda, N., Ide, M., Sano, T., Oyama, T., Tsukagoshi, H., Hamanaka, K., Maeda, M., 2003. Immunohistochemical demonstration of 14-3-3 sigma protein in normal human tissues and lung cancers, and the preponderance of its strong expression in epithelial cells of squamous cell lineage. Pathol. Int. 53, 353–360.

Newcombe, J., Li, H., Cuzner, M.L., 1994. Low density lipoprotein uptake by macrophages in multiple sclerosis plaques: implications for pathogenesis. Neuropathol. Appl. Neurobiol. 20, 152–162.

Nishie, M., Mori, F., Ogawa, M., Sannohe, S., Tanno, K., Kurahashi, K., Kuroda, N., Wakabayashi, K., 2004. Multinucleated astrocytes in old demyelinated plaques in a patient with multiple sclerosis. Neuropathology 24, 248–253.

Satoh, J., Yamamura, T., Arima, K., 2004. The 14-3-3 protein ε isoform expressed in reactive astrocytes in demyelinating lesions of multiple sclerosis binds to vimentin and glial fibrillary acidic protein in cultured human astrocytes. Am. J. Pathol. 165, 577–592.

Satoh, J., Nakanishi, M., Koike, F., Miyake, S., Yamamoto, T., Kawai, M., Kikuchi, S., Nomura, K., Yokoyama, K., Ota, K., Kanda, T., Fukazawa, T., Yamamura, T., 2005. Microarray analysis identifies an aberrant expression of apoptosis and DNA damage-regulatory genes in multiple sclerosis. Neurobiol. Dis. 18, 537–550.

Schlote, W., 1975. Piloid astrocytes (spongiocytes) and Rosenthal fibers in multiple sclerosis. Acta Neuropathol. 33, 35–44.

Schober, A., Böttner, M., Strelau, J., Kinscherf, R., Bonaterra, G.A., Barth, M., Schilling, L., Fairlie, W.D., Breit, S.N., Unsicker, K., 2001. Expression of growth differentiation factor-15/macrophage inhibitory cytokine-1 (GDF-15/MIC-1) in the perinatal, adult, and injured rat brain. J. Comp. Neurol. 439, 32–45.

Slee, E.A., O'Connor, D.J., Lu, X., 2004. To die or not to die: how does p53 decide? Oncogene 23, 2809–2818.

Smith, K.J., Kapoor, R., Felts, P.A., 1999. Demyelination: the role of reactive oxygen and nitrogen species. Brain Pathol. 9, 62–92.

Strelau, J., Sullivan, A., Böttner, M., Lingor, P., Falkenstein, E., Syter-Crazzolara, C., Galter, D., Jaszai, J., Krieglstein, K., Unsicker, K., 2000. Growth/differentiation factor-15/macrophage inhibitory cytokine-1 is a novel trophic factor for midbrain dopaminergic neurons in vivo. J. Neurosci. 20, 8597–8603.

Toyokuni, S., Miyake, N., Hiai, H., Hagiwara, M., Kawakishi, S., Osawa, T., Uchida, K., 1995. The monoclonal antibody specific for the 4-hydroxy-2-nonenal histidine adduct. FEBS Lett. 359, 189–191.

Toyokuni, S., Tanaka, T., Hattori, Y., Nishiyama, Y., Yoshida, A., Uchida, K., Jiai, H., Ochi, H., Osawa, T., 1997. Quantitative immunohistochemical determination of 8-hydroxy-2′-deoxyguanosine by a monoclonal antibody N45.1: its application to ferric nitrilotriacetate-induced renal carcinogenesis model. Lab. Invest. 76, 365–374.

Uchida, K., Shiraishi, M., Naito, Y., Torii, Y., Nakamura, Y., Osawa, T., 1999. Activation of stress signaling pathways by the end product of lipid peroxidation. 4-Hydroxy-2-nonenal is a potential inducer of intracellular peroxide production. J. Biol. Chem. 274, 2234–2242.

Umahara, T., Uchihara, T., Tsuchiya, K., Nakamura, A., Ikeda, K., Iwamoto, T., Takasaki, M., 2004. Immunolocalization of 14-3-3 isoforms in brains with Pick body disease. Neurosci. Lett. 371, 215–219.

Urano, T., Saito, T., Tsukui, T., Fujita, M., Hosoi, T., Muramatsu, M., Ouchi, Y., Inoue, S., 2002. Efp targets 14-3-3σ for proteolysis and promotes breast tumor growth. Nature 417, 871–875.

Urano, T., Takahashi, S., Suzuki, T., Fujimura, T., Fujita, M., Kumagai, J., Horie-Inoue, K., Sasano, H., Kitamura, T., Ouchi, Y., Inoue, S., 2004. 14-3-3σ is down-regulated in human prostate cancer. Biochem. Biophys. Res. Commun. 319, 795–800.

Vladimirova, O., O'Connor, J., Cahil, A., Alder, H., Butunoi, C., Kalman, B., 1998. Oxidative damage to DNA in plaques of MS brains. Mult. Scler. 4, 413–418.

Wang, Y., Barbacioru, C., Hyland, F., Xiao, W., Hunkapiller, K.L., Blake, J., Chan, F., Gonzalez, C., Zhang, L., Samaha, R.R., 2006. Large scale real-time PCR validation on gene expression measurements from two commercial long-oligonucleotide microarrays. BMC Genomics 7, 59 (online).

Yang, H.-Y., Wen, Y.-Y., Chen, C.-H., Lozano, G., Lee, M.-H., 2003. 14-3-3σ positively regulates p53 and suppresses tumor growth. Mol. Cell Biol. 23, 7096–7107.

Zerr, I., Bodemer, M., Gefeller, O., Otto, M., Poser, S., Wiltfang, J., Windl, O., Kretzschmar, H.A., Weber, T., 1998. Detection of 14-3-3 protein in the cerebrospinal fluid supports the diagnosis of Creutzfeldt-Jakob disease. Ann. Neurol. 43, 32–40.

Zhao, R., Gish, K., Murphy, M., Yin, Y., Notterman, D., Hoffman, W.H., Tom, E., Mack, D.H., Levine, A.J., 2000. Analysis of p53-regulated gene expression patterns using oligonucleotide arrays. Genes Dev. 14, 981–993.

Zhou, B.-B.S., Elledge, S.J., 2000. The DNA damage response: putting checkpoints in perspective. Nature 408, 433–439.

Differential Expression of CD11c by Peripheral Blood NK Cells Reflects Temporal Activity of Multiple Sclerosis[1]

Toshimasa Aranami, Sachiko Miyake, and Takashi Yamamura[2]

Multiple sclerosis (MS) is an autoimmune disease, showing a great degree of variance in temporal disease activity. We have recently demonstrated that peripheral blood NK cells biased for secreting IL-5 (NK2 bias) are associated with the remission state of MS. In this study, we report that MS patients in remission differentially express CD11c on NK cell surface (operationally defined as $CD11c^{high}$ or $CD11c^{low}$). When we compared $CD11c^{high}$ or $CD11c^{low}$ patients, the expression of IL-5 and GATA-3 in NK cells supposed to endow a disease-protective NK2 phenotype was observed in $CD11c^{low}$ but not in $CD11c^{high}$ patients. In contrast, the $CD11c^{high}$ group showed a higher expression of HLA-DR on NK cells. In vitro studies demonstrated that NK cell stimulatory cytokines such as IL-15 would up-regulate CD11c expression on NK cells. Given previous evidence showing an association between an increased level of proinflammatory cytokines and temporal disease activity in MS, we postulate that inflammatory signals may play a role in inducing the $CD11c^{high}$ NK cell phenotype. Follow-up of a new cohort of patients showed that 6 of 10 $CD11c^{high}$ MS patients developed a clinical relapse within 120 days after evaluation, whereas only 2 of 13 $CD11c^{low}$ developed exacerbated disease ($p = 0.003$). As such, a higher expression of CD11c on NK cells may reflect the temporal activity of MS as well as a loss of regulatory NK2 phenotype, which may allow us to use it as a potential biomarker to monitor the immunological status of MS patients. *The Journal of Immunology*, **2006, 177: 5659–5667.**

Multiple sclerosis (MS)[3] is a chronic inflammatory disease of the CNS, in which autoreactive T cells targeting CNS Ags are presumed to play a pathogenic role (1). A large majority of the patients with MS (~70%), known as relapsing-remitting MS, would develop acute exacerbations of disease between intervals of remission. It is currently believed that relapses are caused by T cell- and Ab-mediated inflammatory reactions to the self-CNS components, and could be controlled at least to some degree by anti-inflammatory therapeutics, immunosuppressants, or plasma exchange.

The clinical course of MS varies greatly among individuals, implicating difficulties to predict the future of each patient. For example, patients who had been clinically inactive in the early stage of illness could abruptly change into active MS accompanying frequent relapses and progressive worsening of neurological conditions. There are a number of unpredictable matters in MS, including an interval between relapses, responsiveness to remedy and the prognosis in terms of neurological disability. To provide better quality of management of the patients, searches of appropriate biomarkers are currently being warranted (2).

We have recently shown that surface phenotype and cytokine secretion pattern of peripheral blood NK cells may reflect the disease activity of MS (3, 4). A combination of quantitative PCR and flow cytometry analysis has revealed that NK cells in clinical remission of MS are characterized by a higher frequency of $CD95^+$ cells as well as a higher expression level of IL-5 than those of healthy subjects (HS) (3). As IL-5-producing NK cells, referred to as NK2 cells (5), could prohibit Th1 cell activation in vitro (3), we interpreted that the NK2 bias in MS may contribute to maintaining the remission state of MS. More recently, we have found that MS patients in remission can be further divided into $CD95^{high}$ and $CD95^{low}$, according to the frequency of $CD95^+$ cells among NK cells (4). Notably, memory T cells reactive to myelin basic protein, a major target Ag in MS, were increased in $CD95^{high}$ patients, compared with $CD95^{low}$. Of note, $CD95^{high}$ NK cells exhibited an ability to actively suppress the autoimmune T cells, whereas those from $CD95^{low}$ patients did not. These results suggest that NK cells may accommodate their function and phenotype to properly counterregulate autoimmune T cells in the remission state of MS.

Recently, a distinct population of NK cells that express CD11c, a prototypical dendritic cell (DC) marker, was identified in mice (6, 7). As the $CD11c^+$ NK cells exhibited both NK and DC functions, they are called as "bitypic NK/DC cells." CD11c associates with integrin CD18 to form CD11c/CD18 complex and is expressed on monocytes, granulocytes, DCs, and a subset of NK cells. Although precise functions are unclear, it has been reported that CD11c is involved in binding of iC3b (8), adhesion to stimulated endothelium (9) or phagocytosis of apoptotic cells (10). The initial purpose of this study was to evaluate CD11c expression and function of $CD11c^+$ NK cells in MS in the line of our research to characterize NK cells in MS. On initiating study, we noticed that there was no significant difference between MS and HS in the frequency of $CD11c^+$ NK cells. However, expression levels of CD11c were significantly higher in MS. We further noticed that up-regulation of CD11c is seen in some, but not all, patients with MS. So we have operationally classified MS into $CD11c^{low}$ and $CD11c^{high}$.

In this study, we demonstrate that IL-5, characteristic of NK2 cells (5), were significantly down-regulated in $CD11c^{high}$ than

Department of Immunology, National Institute of Neuroscience, National Center of Neurology and Psychiatry, Tokyo, Japan

Received for publication May 3, 2006. Accepted for publication July 28, 2006.

The costs of publication of this article were defrayed in part by the payment of page charges. This article must therefore be hereby marked *advertisement* in accordance with 18 U.S.C. Section 1734 solely to indicate this fact.

[1] This work was supported by grants from the Ministry of Health, Labor and Welfare of Japan and the Program for Promotion of Fundamental Studies in Health Sciences of the National Institute of Biomedical Innovation.

[2] Address correspondence and reprint requests to Dr. Takashi Yamamura, Department of Immunology, National Institute of Neuroscience, National Center of Neurology and Psychiatry, 4-1-1 Ogawahigashi, Kodaira, Tokyo 187-8502, Japan. E-mail address: yamamura@ncnp.go.jp

[3] Abbreviations used in this paper: MS, multiple sclerosis; HS, healthy subject; DC, dendritic cell; MFI, mean fluorescence intensity; ECD, energy-coupled dye.

0022-1767/06/$02.00

$CD11c^{low}$ NK cells. In contrast, expression of HLA-DR class II molecule was up-regulated in $CD11c^{high}$ NK cells. Notably, both CD11c and HLA-DR on NK cells were reproducibly induced in vitro in the presence of IL-15 (11) or combination of inflammatory cytokines, known to be increased in the blood of MS (12–14). Furthermore, we found that the remission state of $CD11c^{high}$ is unstable in comparison to $CD11c^{low}$, as judged by an increased number of the patients who exacerbated during the 120 days after examining NK cell phenotypes. These results suggest that the $CD11c^{high}$ group of patients may be in more unstable condition than $CD11c^{low}$, presenting with reduced regulatory functions of NK cells.

Materials and Methods

Subjects

Twenty-five patients with relapsing-remitting MS (15) (male (M)/female (F) = 8/17; age = 37.7 ± 11.1 (year old)) and 10 sex- and age-matched HS (M/F = 3/7; age = 39.9 ± 12.2 (year old)) were enrolled for studying NK cell phenotypes. All the patients were in the state of remission at examination as judged by magnetic resonance imaging scanning and clinical assessment. They had not been given immunosuppressive medications, or corticosteroid for at least 1 mo before examination. They had relatively mild neurological disability (expanded disability status scale <4) and could walk to the hospital without any assistance during remission. The same neurologist followed up the patients regularly (every 3–4 wk) and judged the occurrence of relapse by using magnetic resonance imaging and clinical examinations. Information on NK cell phenotype or other immunological parameters was never given to either the neurologist or the patients at the time of evaluation. To precisely determine the onset of relapse, patients were allowed to take examination within a few days after a new symptom appeared. Written informed consent was obtained from all the patients and the Ethics Committee of the National Center of Neuroscience (NCNP) approved the study.

Reagents

Mouse IgG1 isotype control-PE, anti-CD3-energy-coupled dye (ECD), anti-CD4-PE, anti-CD8-PC5, anti-CD56-PC5, anti-CD69-PE, and anti-HLA-DR-FITC mAbs were purchased from Immunotech. Anti-CD11c-PE and anti-CD95-FITC were purchased from BD Pharmingen. Recombinant human cytokines were purchased from PeproTech. AIM-V (Invitrogen Life Technologies) was used for cell culture after supplementing 2 mM L-glutamine, 100 U/ml penicillin, and 100 mg/ml streptomycin (Invitrogen Life Technologies).

Cell preparation and NK cell purification

PBMC were separated by density gradient centrifugation with Ficoll-Hypaque PLUS (Amersham Biosciences). To purify NK cells, PBMC were treated with NK isolation kit II (Miltenyi Biotec) twice, according to the manufacturer's protocol. Briefly, PBMC were labeled with a mixture of biotin-conjugated mAbs reactive to non-NK cells and magnetic microbead-conjugated anti-biotin mAbs. The magnetically labeled non-NK cells were depleted with auto-MACS (Miltenyi Biotec) and this procedure always yielded >95% purity of NK cells when assessed by the proportions of $CD3^{-}CD56^{+}$ cells with flow cytometry.

Flow cytometry

To evaluate the expression of CD11c, CD95, or other surface molecules on NK cells, PBMC were stained with anti-CD3-ECD, anti-CD56-PC5, and FITC- or PE-conjugated mAbs against molecules of our interest and were analyzed with EPICS flow cytometry (Beckman Coulter). Mean fluorescence intensity (MFI) of CD11c was measured on gated $CD11c^{+}$ fraction or whole NK cells.

Stimulation of purified NK cells with proinflammatory cytokines

Purified NK cells (1×10^5/well) were stimulated in the presence or absence of IL-4, IL-8, IL-12, IL-15, IL-18, IL-23, TNF-α, and GM-CSF or combination of IL-12, IL-15, and IL-18 for 3 days. We analyzed CD11c expression after staining the cells with anti-CD11c-PE, anti-CD3-ECD, and anti-CD56-PC5. The concentration of IL-12 was at 10 ng/ml, and those of the other cytokines were at 100 ng/ml.

RT-PCR

Total RNA were extracted with a RNeasy Mini kit (Qiagen) from purified NK cells, and the cDNA were synthesized with Super Script III first strand systems (Invitrogen Life Technologies) according to the manufacturer's protocol. For quantitative analysis of IL-5, IFN-γ, GATA-3, and T-bet, the LightCycler quantitative PCR system (Roche Diagnostics) was used. Relative quantities of mRNA were evaluated after normalizing each expression levels with β-actin expression. PCR primers used were as follows: β-actin-sense, AGAGATGGCCACGGCTGCTT, and -antisense, ATTT GCGGTGGACGATGGAG; IFN-γ-sense, CAGGTCATTCAGATGTA GCG, and -antisense, GCTTTTCGAAGTCATCTCG; IL-5-sense, GCA CACTGGAGAGTCAAACT, and -antisense, CACTCGGTGTTCATTA CACC; GATA-3-sense, CTACGGAAACTCGGTCAGG, and -antisense, CTGGTACTTGAGGCACTCTT; T-bet-sense, GGAGGACACCGACTA ATTTGGGA, and -antisense, AAGCAAGACGCAGCACCAGGTAA.

Statistical analysis of remission rate

We set the first episode of relapse after blood sampling as an end point, although we followed clinical course of each patient for up to 120 days, regardless of whether they developed relapses. No patients developed second relapse during the 120 days. When the neurologist prescribed corticosteroids without knowing any information on the NK cell phenotype, the patient was considered as the dropout at that time point. Remission rate was calculated as Kaplan-Meier survival rate, and statistical difference between $CD11c^{low}$ and $CD11c^{high}$ MS was evaluated with the log-rank test.

Results

CD11c on NK cells is up-regulated in MS remission

First, we confirmed that PBMC from healthy individuals and MS contain $CD11c^{+}$ NK cells (Fig. 1), which constitute a major population of whole NK cells. We then noticed that proportion of $CD11c^{+}$ NK cells as well as its levels of expression greatly varied among individuals, particularly in MS. To examine this issue further, we systemically examined 25 MS patients in remission and 10 HS for NK cell expression of CD11c. Whereas 20–80% of NK cells are $CD11c^{+}$ in HS (Fig. 1*c*), almost all NK cells were $CD11c^{+}$ in some MS patients (Fig. 1, *c* and *e*). However, reflecting a great degree of variance, comparison between HS and MS did not reveal a significant difference (Fig. 1*c*). In contrast, when we measured the MFI of CD11c expression on $CD11c^{+}$ NK cells, it was significantly higher in MS as compared with HS (Fig. 1*a*). This difference was also noticed when MFI of CD11c was measured for all the NK cell populations (Fig. 1*b*). It was interesting to know whether the levels of CD11c expression may correlate with NK cell functions. Therefore, we operationally divided the MS patients into $CD11c^{low}$ and $CD11c^{high}$ subgroups (Fig. 1*a*), by setting the border as (the average + 2 × SD) of the values for HS.

$CD11c^{high}$ NK cells express HLA-DR more brightly than $CD11c^{low}$ NK cells

It was previously reported that infection with certain viruses would accompany up-regulation of CD11c on NK cells (16). This raises a possibility that the increased expression of CD11c in $CD11c^{high}$ MS may reflect an activation state of NK cells caused by some sort of stimuli. To verify this hypothesis, we examined surface expression of cell activation markers (CD69 and HLA-DR). Although CD69, an early activation marker, was not detectable on NK cells (Fig. 2*a*), NK cells from MS, particularly $CD11c^{high}$ MS, significantly overexpressed HLA-DR on surface (Fig. 2). Interestingly, HLA-DR expression was also up-regulated on $CD4^{+}$ T cells from $CD11c^{high}$ MS compared with those from HS (data not shown). These results indicate that NK cells and T cells are differentially activated in $CD11c^{high}$ MS, $CD11c^{low}$ MS, and HS.

Absence of NK2 bias in $CD11c^{high}$ MS

We have previously reported that a higher level of IL-5 expression (NK2 bias) is one of the characteristics of NK cells of MS in

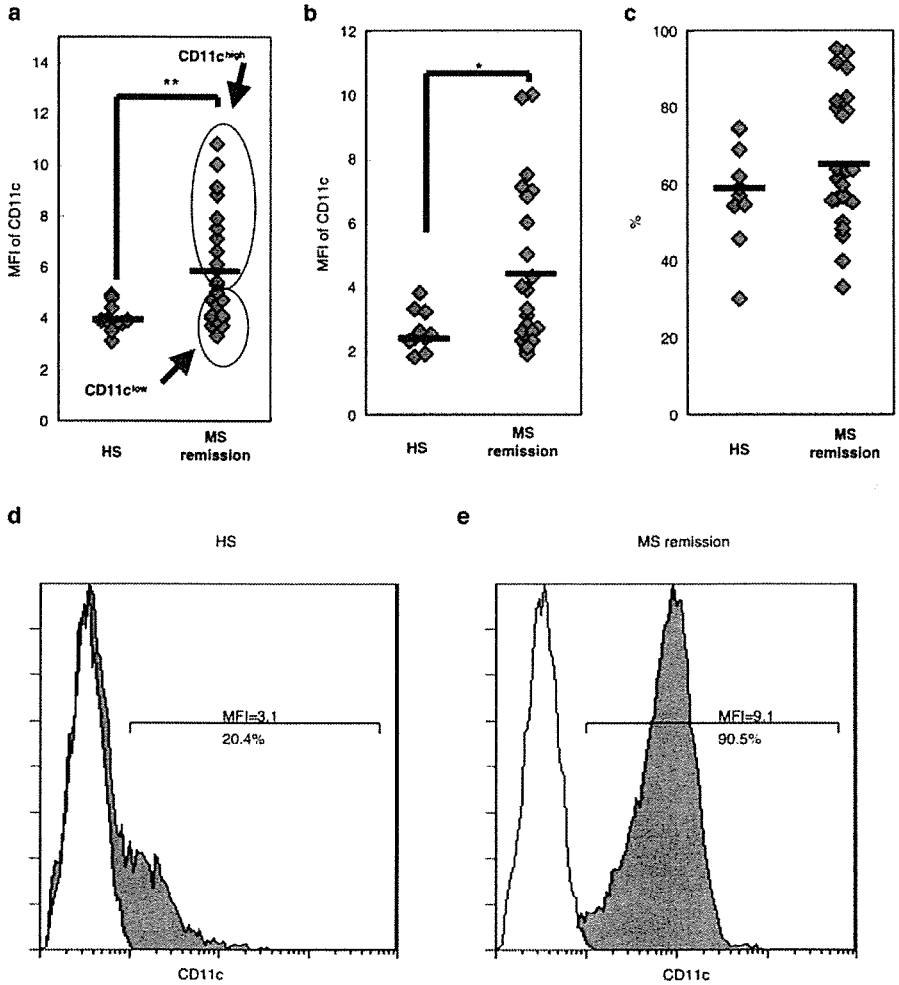

FIGURE 1. CD11c on NK cells is up-regulated in MS in remission. *a*, PBMC from HS (n = 10) and MS patients in remission (n = 25) were stained with anti-CD11c-PE, -CD3-ECD, and -CD56-PC5 mAb, and CD11c expression was measured on the $CD11c^+$ fraction gated within whole NK cells ($CD11c^+CD3^-CD56^+$ cells) as mean fluorescence intensity (MFI). Each dot represents the data from individual patients. $CD11c^{high}$ and $CD11c^{low}$ groups of patients are encircled as described in the text. *b*, In parallel, CD11c expression (MFI) was measured for the whole NK cells ($CD3^-CD56^+$ cells), which yielded a similar result. *c*, The proportions of $CD11c^+$ cells among whole NK cells are plotted. No significant difference was noted between HS and MS remission. *d* and *e*, Representative histogram patterns of CD11c on NK cells (closed histogram) from a single healthy subject (HS) (*d*) and a patient corresponding to $CD11c^{high}$ MS (*e*). Open histograms represent isotype control staining. Values represent proportions of $CD11c^+$ fraction (%) and MFI for $CD11c^+$ cells. Mann-Whitney U test was used for statistical analysis. Horizontal bars indicate the mean values. *, $p < 0.05$; **, $p < 0.01$.

remission (3). Although the mechanism for NK2 bias in MS remains to be further studied, up-regulation of GATA-3 has recently been reported in the induction of NK2 cells in mice (17). To explore the possible difference in the functions of $CD11c^{high}$ and $CD11c^{low}$ NK cells, we isolated NK cells from $CD11c^{high}$ or $CD11c^{low}$ group of patients and measured the mRNA levels of representative cytokines IFN-γ and IL-5 as well as corresponding transcription factors T-bet and GATA-3. As shown in Fig. 3, mRNA expression of both IL-5 and GATA-3 was significantly higher in $CD11c^{low}$ MS compared with HS or $CD11c^{high}$ MS, indicating that NK2 bias thought to be characteristic of MS remission is restricted to $CD11c^{low}$ MS. In contrast, there were no differences in mRNA expression of IFN-γ and T-bet among these three groups. Because NK cells from $CD11c^{high}$ patients expressed HLA-DR most brightly, we speculate that NK2 bias associated with $CD11c^{low}$ MS would attenuate when NK cells are further activated or differentiated.

NK cell stimulatory proinflammatory cytokines induce up-regulation of CD11c

We next attempted to explore the mechanism(s) for up-regulation of CD11c on NK cells in $CD11c^{high}$ MS. Because both NK cells and $CD4^+$ T cells overexpressed HLA-DR in $CD11c^{high}$, is it probable that immune signals influencing both innate and acquired immunity are operative. So we hypothesized that cytokine signals that have been implicated in the pathogenesis of MS may play a role. We cultured NK cells from HS in the presence or absence of cytokine(s) for 3 days, and evaluated the CD11c expression (MFI). We focused our attention to IL-12, IL-15, and IL-18, which are known to stimulate NK cells with or without help of other cytokines. Notably, they are reportedly elevated in the serum or blood lymphocytes of MS patients as compared with HS (11–14, 18, 19), and prior studies suggest that they may play an important role in autoimmune diseases (20–24). As shown in Fig. 4, although IL-12 and IL-18 showed only a marginal effect on purified NK cells, IL-15 consistently induced 2- to 3-fold up-regulation of CD11c compared with control culture without addition of cytokines. As IL-12 and IL-18 were reported to synergistically work in various settings (25, 26), we then examined whether combinations of these cytokines may induce CD11c. Combination of IL-15 and IL-12 or of IL-15 and IL-18 did not augment the CD11c expression to the level higher than that could be induced by IL-15 alone. However, the combination of IL-12 and IL-18 did up-regulate CD11c on NK cells, which was comparable to the effect of IL-15 alone (Table I). Additionally, we tested the effects of several cytokines involved in differentiation of DC (TNF-α, GM-CSF, IL-4) (27), or known to up-regulate CD11c in granulocytes (IL-8) as controls (28) in the same assay. These cytokines showed no significant effect (Table I).

$CD11c^{high}$ MS relapsed earlier

Given the significant difference in activation status and cytokine phenotype of NK cells as well as HLA-DR expression by $CD4^+$ T cells, it was particularly interesting to know whether $CD11c^{low}$ and $CD11c^{high}$ MS may follow a different clinical course. A new cohort of

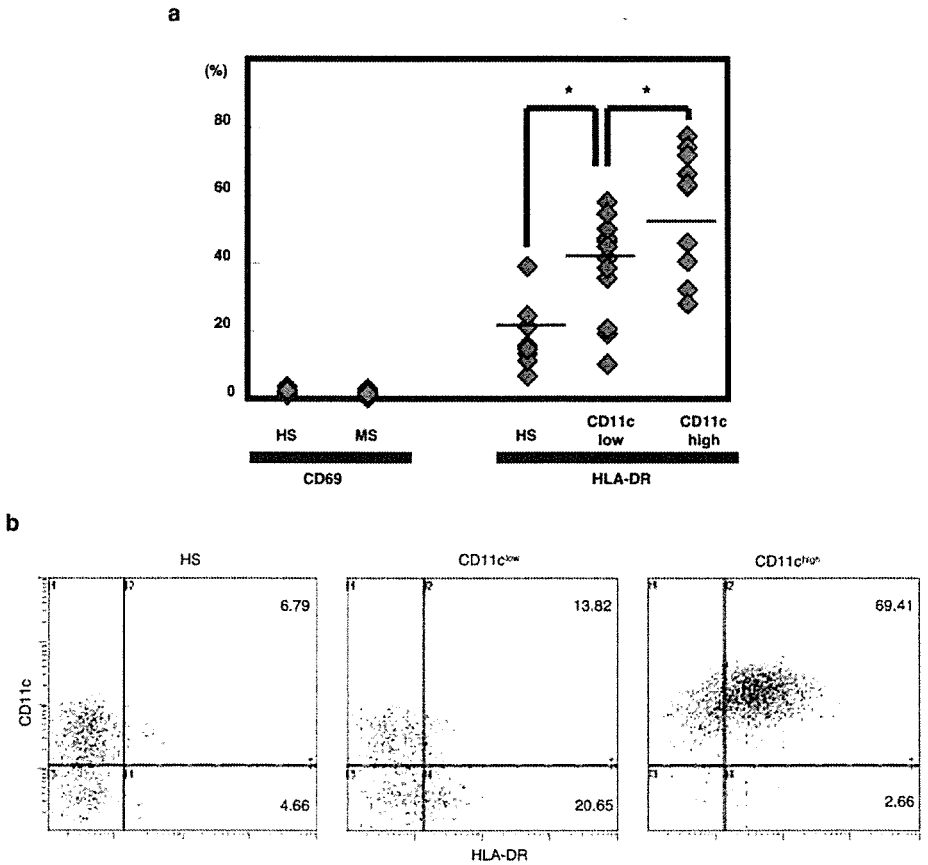

FIGURE 2. Proportions of HLA-DR$^+$ NK cells increase in CD11c^{high} MS. *a*, CD69 and HLA-DR expression on NK cells (CD3$^-$ CD56$^+$ cells). Data are expressed as proportions (percent) of CD69$^+$ cells (7 HS and 16 MS patients in remission) or HLA-DR$^+$ cells (10 HS and 25 MS patients) within whole NK cells. The Student *t* test was used for statistical analysis. Horizontal bars indicate the mean values. *, $p < 0.05$. *b*, Representative expression patterns of HLA-DR vs CD11c on NK cells from a healthy subject (*left*), CD11c^{low} MS (*middle*), and CD11c^{high} MS (*right*).

13 CD11c^{low} and 10 CD11c^{high} MS patients listed in Table II were followed for up to 120 days. In this preliminary exploration, we set the first episode of relapse after blood sampling as an end point. When the neurologist prescribed corticosteroids without knowing any information on the NK cell phenotype, the patient was considered as the dropout at that time point. Remission rate was calculated as Kaplan-Meier survival rate, and statistical difference between CD11c^{low} and CD11c^{high} MS was evaluated with the log-rank test (Fig. 5*a*). At entry, there was no significant difference in the age and disease duration between CD11c^{low} and CD11c^{high} MS (Table II). On analyzing the collected data after completing the study, we found that 8 patients developed a single relapse during the observation period and that the proportion of patients who have had relapse during the follow-up period was greatly higher in CD11c^{high} MS (6 of 10, 60%) than in CD11c^{low} MS (2 of 13, 15.3%). Furthermore, the log-rank test revealed that CD11c^{high} MS relapsed significantly earlier than CD11c^{low} MS ($p = 0.003$), suggesting a possible role of CD11c as a temporal marker for predicting relapse within months after examination. We also explored whether the difference between CD11c^{high} and CD11c^{low} could be influenced by age or sex. When we selected a group of patients younger than 38.5 years old (the mean age of all the patients), a significantly earlier relapse in CD11c^{high} than CD11c^{low} MS was confirmed in this group of patients ($p = 0.0067$, Fig. 5*b*). In the rest of the patients (<38.5 years old), the difference was less clear and not significant ($p = 0.095$). In female patients, CD11c^{high} MS relapsed significantly earlier than CD11c^{low} MS ($p = 0.035$, Fig. 5*c*), whereas this tendency was not statistically significant in male patients ($p = 0.083$). By examining the patients' medical records, we also found that the duration from the last relapse tended to be shorter in CD11c^{high} than CD11c^{low} MS (14.7 ± 12 mo in CD11c^{high} vs 26.7 ± 24.3 mo in CD11c^{low}) and that the mean number of relapses per year was higher in CD11c^{high} MS (0.9 ± 0.6 in CD11c^{high} vs 0.5 ± 0.5 in CD11c^{low}). These are consistent with the postulate that CD11c^{high} MS might be immunologically more active than CD11c^{low} MS (Table II).

Alteration of CD11c expression in the course of MS

We previously described that NK cells may lose NK2 phenotype during relapse (3). It is interesting to know whether the CD11c phenotype also changes in the course of MS. During the follow-up period of 120 days, 8 patients developed a relapse. We were able to take blood samples at relapse before treatment with corticosteroid and then compared the relapse samples with the samples obtained during remission at initiation of the study. As shown in Fig. 6, we saw an obvious tendency that the levels of CD11c expression would decline during relapse ($p < 0.05$). HLA-DR expression on NK cells was also reduced in some patients during relapse, but the difference between remission and relapse samples was not statistically significant.

Expression pattern of CD95 vs CD11c on NK cells in MS

In a previous study, we showed that MS patients could be divided into CD95^{high} and CD95^{low} according to the frequency of CD95$^+$ cells among NK cells (4). Additionally, we examined whether expression of CD11c and CD95 may independently reflect the status of MS. We found no significant correlation between CD95 (%) and CD11c (MFI) on NK cells in MS ($r = 0.29$, $p = 0.16$ with Spearman's correlation coefficient by rank test), indicating that expression of CD95 and CD11c on NK cells may be regulated independently. By setting the upper limits of CD95$^+$ (%) and CD11c MFI as (the average + 2 × SD) of HS (CD95: 44.6%, CD11c: 5.04),

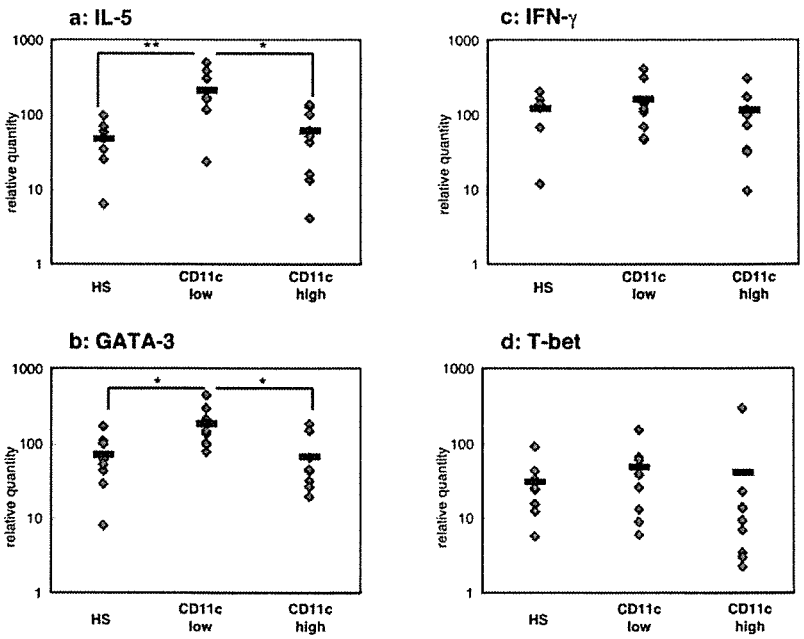

FIGURE 3. IL-5 and GATA-3 mRNA are increased in $CD11c^{low}$ but not in $CD11c^{high}$ MS. Total RNAs were extracted from purified NK cells of HS ($n = 8$), $CD11c^{low}$ ($n = 9$), or $CD11c^{high}$ MS ($n = 8$). mRNA expression of IL-5 (*a*), GATA-3 (*b*), IFN-γ (*c*), and T-bet (*d*) was evaluated by quantitative PCR. The data are normalized to endogenous β-actin expressions in the same samples. ANOVA was used for statistical analysis. Horizontal bars indicate the mean values. *, $p < 0.05$; **, $p < 0.01$.

we then examined whether there is a correlation between CD11c CD95 phenotype and clinical conditions (Fig. 7). Naturally, all the healthy subjects were plotted in the *left lower quadrant* ($CD95^{low}CD11c^{low}$). In contrast, MS patients were plotted in all the four quadrants with differential proportions of patients who have no relapse during 120 days: $CD95^{low}CD11c^{low}$; 3/3 (100%), $CD95^{low}CD11c^{high}$; 1/2 (50%), $CD95^{high}CD11c^{low}$; 8/10 (80%), $CD95^{high}CD11c^{high}$; 2/7 (28.6%). Although the data for $CD95^{low}$ subjects (*lower left* and *lower right*) need to be omitted due to the limited sample size, we found that the difference between $CD95^{high}CD11c^{low}$ and $CD95^{high}CD11c^{high}$ in remission rate was significant with log-rank test ($p = 0.028$). Provided that $CD95^{high}$ patients possessed an increased frequency of memory autoreactive T cells (4), this result is consistent with the idea that when comparable numbers of autoimmune T cells are present in the peripheral circulation, remission of MS is more stable in patients with $CD11c^{low}$ NK cells.

Discussion

Blood examination of systemic autoimmune diseases such as systemic lupus erythematosus usually exhibits measurable abnormalities such as elevation of autoantibodies, which is useful for evaluating activity of disease. In contrast, patients with MS do not accompany such systemic abnormalities in laboratory tests except

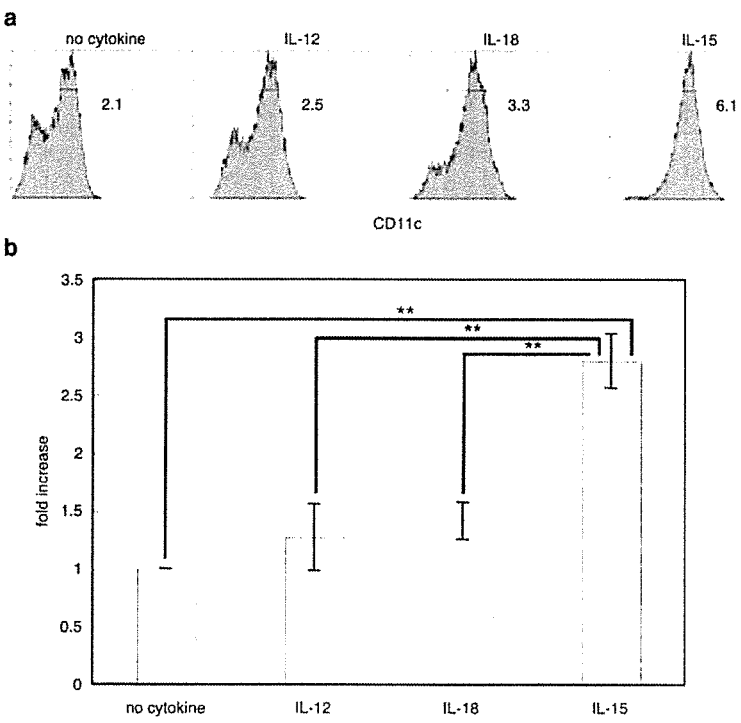

FIGURE 4. CD11c expression on NK cells is upregulated with addition of IL-15. *a*, Purified NK cells were cultured in the absence or presence of IL-12, IL-18, or IL-15. Three days later, the cells were stained with anti-CD11c-PE, -CD3-ECD, and -CD56-PC5 mAb. CD11c expression on NK cells ($CD3^-CD56^+$ cells) is demonstrated as single histogram. Values indicate CD11c MFI of $CD11c^+$ fractions. A representative of three independent experiments is shown. *b*, Data are expressed as mean fold increase of CD11c MFI (the MFI in the presence of cytokine/the MFI in the absence of cytokine) + SD from three independent experiments. ANOVA was used for statistical analysis. **, $p < 0.01$.

Table I. *Effect of several cytokines on CD11c expression on NK cells*

	No Cytokine	IL-12	IL-18	IL-15	IL-12 + IL-18	IL-4	TNF	GM-CSF	IL-23	IL-8
Expt. 1	1.00[a]	1.19	1.57	**2.90**	ND	ND	ND	ND	ND	ND
Expt. 2	1.00	1.04	1.43	**2.96**	**2.86**	ND	ND	ND	ND	ND
Expt. 3	1.00	1.59	1.25	**2.53**	**3.44**	ND	ND	ND	ND	ND
Expt. 4	1.00	ND	ND	**2.62**	ND	1.19	1.10	0.95	1.14	ND
Expt. 5	1.00	ND	ND	**2.81**	ND	1.24	ND	1.05	1.05	1.00
Mean	1.00	1.27	1.42	**2.77**	**3.15**	1.21	1.10	1.00	1.10	1.00
SD	0.00	0.29	0.16	0.19	0.41	0.03		0.07	0.07	

[a] Purified NK cells were stimulated with cytokines. Data are expressed as fold increase of CD11c MFI (the MFI in the presence of the indicated cytokines/the MFI in the absence of cytokines) in the presence of indicated cytokines. More than a 2-fold increase is highlighted (bold).

in unusual cases. It is currently recognized that autoreactive T cells might be activated and expanded to various degrees in the peripheral blood and peripheral lymphoid organs of MS even during remission (1–4). In fact, our previous work suggests that a higher number of memory autoreactive T cells is linked with unstable disease course (4). If we are able to accurately evaluate the immune status of each patient with a relatively simple test, it should be most helpful in treatment and management of MS. In this line, it is currently of particular importance to identify measurable indicators which would serve as clinically appropriate biomarkers in MS (2).

This study has clarified for the first time to our knowledge that CD11c expression on peripheral NK cells is significantly up-regulated in a major proportion of patients with MS in remission. To obtain insights into the mechanism and the biological meaning of the NK cell expression of CD11c in autoimmune disease MS, we have attempted to clarify the difference between $CD11c^{high}$ and $CD11c^{low}$ patients regarding phenotypes of NK cells, cytokine profile, and temporal clinical activity. We also explored which inflammatory cytokines might induce CD11c on NK cells. According to the NK cell expression of CD11c, we have classified the patients with MS in remission into $CD11c^{high}$ and $CD11c^{low}$. Most notably, NK2 phenotype characterized by predominant IL-5 production was seen in $CD11c^{low}$ patients, but not in $CD11c^{high}$. Consistently, the $CD11c^{high}$ patients were found to be clinically more active than $CD11c^{low}$ as judged by the remission rate during the 120 days after examination. These results indicate that up-regulation of CD11c on NK cells would reflect the temporal disease activity and therefore could be used to identify patients who are likely to exacerbate within months. It has been reported that $CD11c^{+}$ NK cells in mice could serve as APCs (6, 7). However, we could not reveal Ag presenting capacity of human $CD11c^{+}$ NK cells (data not shown).

Regarding the mechanism of CD11c induction on NK cells, we have found that in $CD11c^{high}$ patients, HLA-DR is concomitantly up-regulated with CD11c on NK cells (Fig. 2), which suggests that up-regulation of CD11c may represent an activation-induced change. After exploring the culture condition that may induce CD11c on NK cells, we have found that the addition of IL-15 or combination of IL-12 and IL-18 would increase the expression levels of CD11c on NK cells from healthy individuals. Because increased levels of these proinflammatory cytokines are detected in the blood samples of MS (11–13, 18, 19, 23), it is possible that in

Table II. *Information on the patients whose clinical courses were followed for up to 120 days*

Identification No.	Group	Age (years)	Sex	Disease Period (Years)	Total Number of Relapses	Duration from the Last Relapse (mo)	Mean Numbers of Relapse/Year
1	Low	17	F[a]	9.6	2	24	0.2
2	Low	52	M	12.2	9	3	0.7
3	Low	31	F	6.2	13	7	2.1
4	Low	32	F	3.9	1	34	0.3
5	Low	42	F	2.2	1	8	0.5
6	Low	35	M	20	3	88	0.2
7	Low	37	M	8.5	3	50	0.4
8	Low	35	F	2.4	1	38	0.4
9	Low	26	F	4.8	2	10	0.4
10	Low	26	F	1.5	1	8	0.7
11	Low	41	M	5.5	1	24	0.2
12	Low	64	F	4.5	2	8	0.4
13	Low	42	F	6.3	1	45	0.2
Mean + SD		36.9 + 12.0		6.7 + 5.0	3.1 + 3.7	26.7 + 24.3	0.5 + 0.5
14	High	39	M	4.4	2	22	0.5
15	High	31	F	9.2	11	14	1.2
16	High	46	F	7.4	>20[b]	2	ND
17	High	53	F	2.1	4	5	1.9
18	High	59	F	4.9	2	19	0.4
19	High	27	M	9.3	4	9	0.4
20	High	36	F	2.7	1	19	0.4
21	High	34	F	3.8	2	43	0.5
22	High	60	F	3.4	6	10	1.8
23	High	21	F	1.8	2	4	1.1
		40.6 + 13.4		4.9 + 2.8	3.8 + 3.1	14.7 + 12.0	0.9 + 0.6

[a] F, Female; M, male.
[b] This value is eliminated from calculation of the mean.

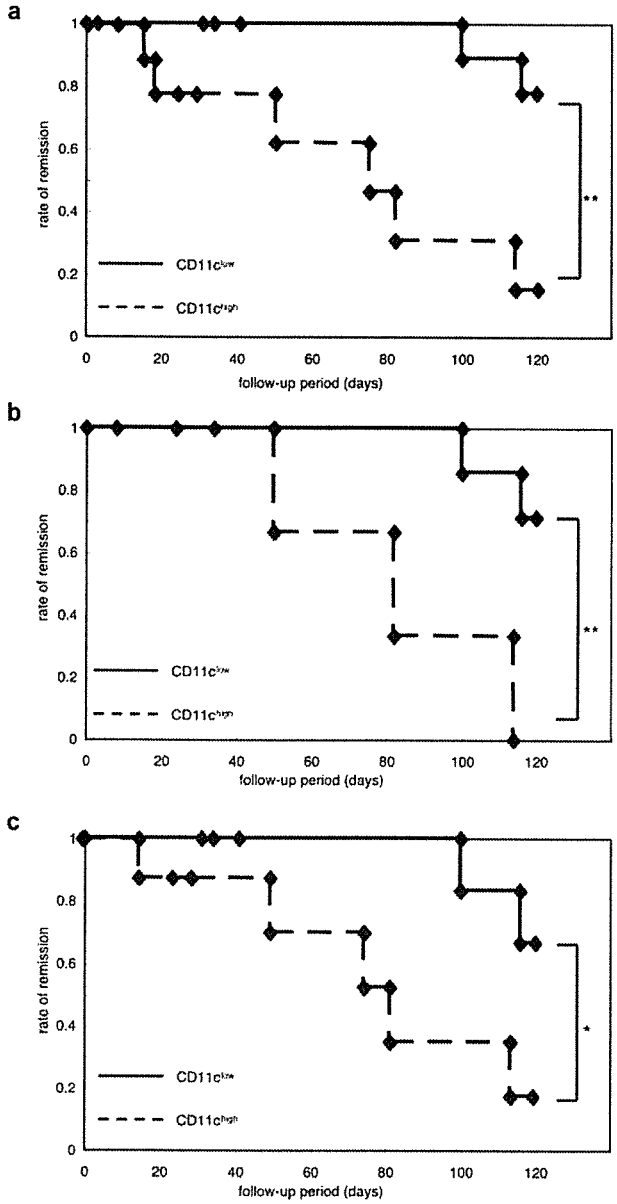

FIGURE 5. Rate of remission is lower in $CD11c^{high}$ MS. The first episode of relapse after blood sampling was set as an end point and clinical course of each patient was followed for up to 120 days. The remission rate was calculated in all (*a*), the younger (*b*), or female (*c*) patients as Kaplan-Meier survival rate, and statistical difference between $CD11c^{low}$ and $CD11c^{high}$ MS was evaluated with log-rank test at day 120. *, $p < 0.05$; **, $p < 0.01$.

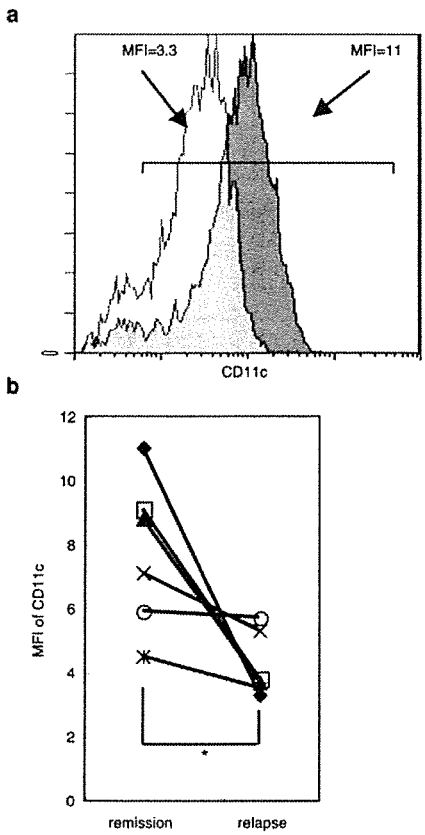

FIGURE 6. Down-regulation of CD11c expression during relapse. *a*, Representative CD11c histograms from the same patient in remission (closed) and relapse (open). Values indicate CD11c MFI of $CD11c^+$ fractions. *b*, Comparison of NK cells from remission and relapse from the same patients ($n = 6$). The data obtained from the same patients are connected with lines. Wilcoxon signed-ranks test was used for statistical analysis. *, $p < 0.05$.

vitro CD11c induction on NK cells may recapitulate the phenotypic alteration of NK cells in $CD11c^{high}$ patients. Interestingly, IL-18 is not only a cytokine able to facilitate IFN-γ production by NK cells in cooperation with IL-12 (25, 26) but is crucial in inducing pathogenic autoimmune responses (21). Furthermore, autoimmune encephalitogenic T cells can induce more serious disease upon adoptive transfer when they are preactivated in the presence of IL-12 and IL-18 (20). Taken together, these results allow us to speculate that the proinflammatory cytokines may be involved in the up-regulation of CD11c on NK cells. Although the relationship between serum cytokine concentration and levels of CD11c expression on NK cells should be estimated in future studies, a previous work (11, 29, 30) showing that a probable link between IL-15 and temporal disease activity, indicates that NK cell expression of CD11c is likely to correlate with the levels of cytokines.

In the Th cell differentiation, specific transcription factors have been identified that play a crucial role in inducing Th1 or Th2 cells. Namely, Th1 differentiation characterized by IFN-γ induction requires a transcription factor T-bet, whereas GATA-3 and c-*maf* act to promote Th2 cytokine production (31–33). Human NK cells cultured in the presence of IL-12 or IL-4 differentiate into NK1 or NK2 populations, reminiscent of Th1 and Th2 cells (5). Whereas NK1 cells produce IL-10 and IFN-γ, NK2 cells would serve as immune regulators by producing IL-5 and IL-13. Notably, up-regulation of GATA-3 has been reported in mouse NK2 cells (17), raising a possibility that Th cells and NK cells might share the same transcription factor for inducing the key cytokine. We have previously reported that IL-5 expression is one of the characteristics of NK cells in the remission state of MS (3). However, it was not excluded that overexpression of IL-5 could be restricted to a proportion of the patients. Here, we have addressed whether NK cells from $CD11c^{high}$ and $CD11c^{low}$ may differ with regard to expression levels of IFN-γ and IL-5 and of their transcription factors T-bet and GATA-3. By measuring the mRNAs, we found that expression levels of IL-5 and GATA-3 are elevated in $CD11c^{low}$ MS but not in $CD11c^{high}$ (Fig. 3). Furthermore, we showed that

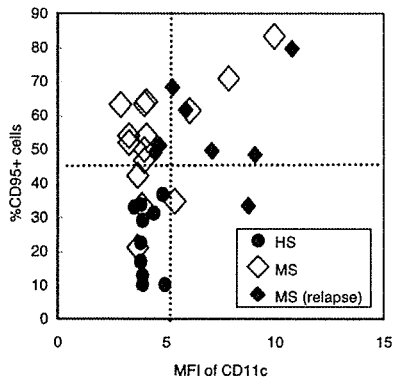

FIGURE 7. Expression pattern of CD95 vs CD11c on NK cells from MS. PBMC from MS or HS were stained with CD95-FITC, CD11c-PE, CD3-ECD, and CD56-PC5. After determining the proportion of $CD95^+$ cells among NK cells and CD11c expression (MFI) of CD11c, we plotted each patient according to the obtained values. Dotted lines represent the upper limits of $CD95^+$ cell (percent) and CD11c MFI for HS as (the average + two times SD) of HS. ●, HS; ◇, MS; ◆, MS patients who relapsed during the 120 days follow-up period.

neither IFN-γ nor T-bet was increased in $CD11c^{high}$ MS. This suggests that NK cells from $CD11c^{low}$ are NK2-biased but those from $CD11c^{high}$ are not, although MS in remission as a whole is NK2-biased as compared with control subjects. More recently, we have observed that stimulation with IL-15 or IL-12 plus IL-18 would decrease IL-5 and GATA-3 mRNA in purified NK cells with reciprocal up-regulation of CD11c (data not shown). This further supports a model that proinflammatory cytokines may play a crucial role in the absence of NK2 bias in $CD11c^{high}$ MS.

To clarify the clinical differences between $CD11c^{high}$ and $CD11c^{low}$, we followed up the clinical course of the patients after blood sampling. Although there was no significant difference in clinical parameters at examination of NK cells, we have found that $CD11c^{high}$ MS showed a significantly earlier relapse than $CD11c^{low}$ MS. This is consistent with our assumption that the absence of NK2 bias in $CD11c^{high}$ MS should imply that regulatory NK cell functions are defective in this group of patients. When we reanalyzed the data regarding various clinical parameters, we found that an earlier relapse in $CD11c^{high}$ than $CD11c^{low}$ MS is more remarkable in the younger group (<38.5 years old) or in female patients. Furthermore, the duration from the last relapse tended to be shorter and the mean number of relapses per year higher in $CD11c^{high}$ MS, supporting that $CD11c^{high}$ MS is more active than $CD11c^{low}$ MS.

When we analyzed expression of CD95 and CD11c on NK cells simultaneously, we found that MS patients in remission could be divided into four subgroups (Fig. 7). When we compared clinical course after examination of NK cell phenotypes, we found that $CD95^{high}CD11c^{high}$ MS relapsed significantly earlier than $CD95^{high}CD11c^{low}$ MS ($p = 0.028$ with log-rank test). This result indicates that $CD95^{high}CD11c^{high}$ MS may be most unstable subgroup of MS, among the patients whose clinical state could be judged as being in clinical remission.

In this study, we have demonstrated that MS patients differentially express CD11c on peripheral blood NK cells and a higher expression of CD11c on NK cells may reflect the temporal disease activity as well as functional alteration of regulatory NK cells. Our results have a clinical implication because of a lack of appropriate biomarker to monitor the immunological status in MS at present. To verify the reliability of this marker, longitudinal examination of CD11c expression on NK cells in the same patients should be performed in the future study.

Disclosures

The authors have no financial conflict of interest.

References

1. Sospedra, M., and R. Martin. 2005. Immunology of multiple sclerosis. *Annu. Rev. Immunol.* 23: 683–747.
2. Bielekova, B., and R. Martin. 2004. Development of biomarkers in multiple sclerosis. *Brain* 127: 1463–1478.
3. Takahashi, K., S. Miyake, T. Kondo, K. Terao, M. Hatakenaka, S. Hashimoto, and T. Yamamura. 2001. Natural killer type 2 bias in remission of multiple sclerosis. *J. Clin. Invest.* 107: R23–R29.
4. Takahashi, K., T. Aranami, M. Endoh, S. Miyake, and T. Yamamura. 2004. The regulatory role of natural killer cells in multiple sclerosis. *Brain* 127: 1917–1927.
5. Peritt, D., S. Robertson, G. Gri, L. Showe, M. Aste-Amezaga, and G. Trinchieri. 1998. Differentiation of human NK cells into NK1 and NK2 subsets. *J. Immunol.* 161: 5821–5824.
6. Homann, D., A. Jahreis, T. Wolfe, A. Hughes, B. Coon, M. J. van Stipdonk, K. R. Prilliman, S. P. Schoenberger, and M. G. von Herrath. 2002. CD40L blockade prevents autoimmune diabetes by induction of bitypic NK/DC regulatory cells. *Immunity* 16: 403–415.
7. Pillarisetty, V. G., S. C. Katz, J. I. Bleier, A. B. Shah, and R. P. Dematteo. 2005. Natural killer dendritic cells have both antigen presenting and lytic function and in response to CpG produce IFN-γ via autocrine IL-12. *J. Immunol.* 174: 2612–2618.
8. Bilsland, C. A., M. S. Diamond, and T. A. Springer. 1994. The leukocyte integrin p150,95 (CD11c/CD18) as a receptor for iC3b: activation by a heterologous β subunit and localization of a ligand recognition site to the I domain. *J. Immunol.* 152: 4582–4589.
9. Stacker, S. A., and T. A. Springer. 1991. Leukocyte integrin P150,95 (CD11c/CD18) functions as an adhesion molecule binding to a counter-receptor on stimulated endothelium. *J. Immunol.* 146: 648–655.
10. Morelli, A. E., A. T. Larregina, W. J. Shufesky, A. F. Zahorchak, A. J. Logar, G. D. Papworth, Z. Wang, S. C. Watkins, L. D. Falo, Jr., and A. W. Thomson. 2003. Internalization of circulating apoptotic cells by splenic marginal zone dendritic cells: dependence on complement receptors and effect on cytokine production. *Blood* 101: 611–620.
11. Blanco-Jerez, C., J. F. Plaza, J. Masjuan, L. M. Orensanz, and J. C. Alvarez-Cermeno. 2002. Increased levels of IL-15 mRNA in relapsing-remitting multiple sclerosis attacks. *J. Neuroimmunol.* 128: 90–94.
12. Huang, W. X., P. Huang, and J. Hillert. 2004. Increased expression of caspase-1 and interleukin-18 in peripheral blood mononuclear cells in patients with multiple sclerosis. *Mult. Scler.* 10: 482–487.
13. Balashov, K. E., D. R. Smith, S. J. Khoury, D. A. Hafler, and H. L. Weiner. 1997. Increased interleukin 12 production in progressive multiple sclerosis: induction by activated $CD4^+$ T cells via CD40 ligand. *Proc. Natl. Acad. Sci. USA* 94: 599–603.
14. Karni, A., D. N. Koldzic, P. Bharanidharan, S. J. Khoury, and H. L. Weiner. 2002. IL-18 is linked to raised IFN-γ in multiple sclerosis and is induced by activated $CD4^+$ T cells via CD40-CD40 ligand interactions. *J. Neuroimmunol.* 125: 134–140.
15. McDonald, W. I., A. Compston, G. Edan, D. Goodkin, H. P. Hartung, F. D. Lublin, H. F. McFarland, D. W. Paty, C. H. Polman, S. C. Reingold, et al. 2001. Recommended diagnostic criteria for multiple sclerosis: guidelines from the International Panel on the diagnosis of multiple sclerosis. *Ann. Neurol.* 50: 121–127.
16. Lima, M., J. Almeida, M. dos Anjos Teixeira, M. L. Queiros, B. Justica, and A. Orfao. 2002. The "ex vivo" patterns of CD2/CD7, CD57/CD11c, CD38/CD11b, CD45RA/CD45RO, and CD11a/HLA-DR expression identify acute/early and chronic/late NK-cell activation states. *Blood Cells Mol. Dis.* 28: 181–190.
17. Katsumoto, T., M. Kimura, M. Yamashita, H. Hosokawa, K. Hashimoto, A. Hasegawa, M. Omori, T. Miyamoto, M. Taniguchi, and T. Nakayama. 2004. STAT6-dependent differentiation and production of IL-5 and IL-13 in murine NK2 cells. *J. Immunol.* 173: 4967–4975.
18. Nicoletti, F., R. Di Marco, K. Mangano, F. Patti, E. Reggio, A. Nicoletti, K. Bendtzen, and A. Reggio. 2001. Increased serum levels of interleukin-18 in patients with multiple sclerosis. *Neurology* 57: 342–344.
19. Fassbender, K., A. Ragoschke, S. Rossol, A. Schwartz, O. Mielke, A. Paulig, and M. Hennerici. 1998. Increased release of interleukin-12p40 in MS: association with intracerebral inflammation. *Neurology* 51: 753–758.
20. Ito, A., A. Matejuk, C. Hopke, H. Drought, J. Dwyer, A. Zamora, S. Subramanian, A. A. Vandenbark, and H. Offner. 2003. Transfer of severe experimental autoimmune encephalomyelitis by IL-12- and IL-18-potentiated T cells is estrogen sensitive. *J. Immunol.* 170: 4802–4809.
21. Shi, F. D., K. Takeda, S. Akira, N. Sarvetnick, and H. G. Ljunggren. 2000. IL-18 directs autoreactive T cells and promotes autodestruction in the central nervous system via induction of IFN-γ by NK cells. *J. Immunol.* 165: 3099–3104.
22. Takeda, K., H. Tsutsui, T. Yoshimoto, O. Adachi, N. Yoshida, T. Kishimoto, H. Okamura, K. Nakanishi, and S. Akira. 1998. Defective NK cell activity and Th1 response in IL-18-deficient mice. *Immunity* 8: 383–390.